

Cosmic Microwave Background and the issue of a fundamental preferred frame

M. Consoli^(a) and A. Pluchino^(b,a)

a) Istituto Nazionale di Fisica Nucleare, Sezione di Catania, Italy

b) Dipartimento di Fisica e Astronomia dell'Università di Catania, Italy

Abstract

The possibility to correlate ether-drift measurements in laboratory and direct CMB observations with satellites in space would definitely confirm the existence of a fundamental preferred frame for relativity. Today, the small residuals observed so far (from Michelson-Morley onward) are just considered typical instrumental effects in experiments with better and better sensitivity. Though, if the velocity of light propagating in the various interferometers is not exactly the same parameter c of Lorentz transformations, nothing would really prevent to observe an ether drift. Thus, for the earth cosmic velocity $v=370$ km/s, we argue that a fundamental 10^{-15} light anisotropy, as presently observed in vacuum and in solid dielectrics, is revealing a 10^{-9} difference in the effective vacuum refractivity between an apparatus in an ideal freely-falling frame and an apparatus on the earth surface. In this perspective, the stochastic nature of the physical vacuum could also explain the irregular character of the signal and the observed substantial reduction from its instantaneous 10^{-15} value to its statistical average 10^{-18} (or smaller). For the same $v=370$ km/s the different refractivities, respectively $\mathcal{O}(10^{-4})$ and $\mathcal{O}(10^{-5})$ for air or helium at atmospheric pressure, could also explain the observed light anisotropy, respectively $\mathcal{O}(10^{-10})$ and $\mathcal{O}(10^{-11})$. However, for consistency, one should also understand the physical mechanism which enhances the signal in weakly bound gaseous matter but remains ineffective in solid dielectrics where the refractivity is $\mathcal{O}(1)$. This mechanism is naturally identified in a non-local, tiny temperature gradient of a fraction of millikelvin which is found in all classical experiments and might ultimately be related to the CMB temperature dipole of ± 3 mK or reflect the fundamental energy flow associated with a Lorentz-non-invariant vacuum state. The importance of the issue would deserve more stringent tests with dedicated experiments and significant improvements in the data analysis.

PACS: 03.30.+p; 98.70.Vc; 11.30.Cp; 07.60.Ly

1. Introduction

1.1 CMB and the issue of a fundamental preferred frame

Precise observations with satellites in space have revealed a tiny anisotropy in the temperature of the Cosmic Microwave Background (CMB) [1, 2]. The present interpretation of its dominant dipole component (the *kinematic* dipole [3]) is in terms of a Doppler effect ($\beta = v/c$)

$$T(\theta) = \frac{T_o \sqrt{1 - \beta^2}}{1 - \beta \cos \theta} \quad (1)$$

due to a motion of the solar system with average velocity $v \sim 370$ km/s toward a point in the sky of right ascension $\alpha \sim 168^\circ$ and declination $\gamma \sim -7^\circ$. Therefore, if one sets $T_o \sim 2.7$ K and $\beta \sim 0.0012$, as for $v \sim 370$ km/s, there are angular variations of a few millikelvin

$$\Delta T(\theta) \sim T_o \beta \cos \theta \sim \pm 3 \text{ mK} \quad (2)$$

By accepting this interpretation, the question naturally arises concerning the role of the system where the CMB dipole anisotropy vanishes exactly, i.e. does it represent a fundamental frame for relativity? The usual answer is that the two concepts are unrelated. Namely, the CMB is a definite medium with a rest frame where the dipole anisotropy is zero. Motion with respect to this frame can be detected and, in fact, has been detected. But the existence of a fundamental preferred frame would contradict special relativity which is the presently accepted interpretation of the theory.

Still, it should not be overlooked that the observed CMB dipole can be reconstructed, to good approximation, by combining the various peculiar motions which are involved, namely the rotation of the solar system around the galactic center, the motion of the Milky Way around the center of the Local Group and the motion of the Local Group of galaxies in the direction of that large concentration of matter known as the Great Attractor [2]. In this way, once a vanishing CMB dipole is equivalent to switching-off all possible peculiar motions, one naturally arrives to the concept of a global frame of rest determined by the average distribution of matter in the universe.

At the same time, at a more formal level, the idea of a preferred frame finds other motivations in the modern picture of the vacuum, intended as the lowest energy state of the theory. This is believed to arise from the macroscopic condensation process, see e.g. [4, 5, 6], of elementary quanta (Higgs particles, quark-antiquark pairs, gluons...) in the same zero-3-momentum state and thus, by definition, singles out some reference frame Σ . Then, the fundamental question [6] is how to reconcile this picture with a basic postulate of axiomatic quantum field theory: the exact Lorentz invariance of the vacuum [7].

Usually this is not considered as a problem with the motivation, perhaps, that the average properties of the condensed phase are summarized into a single quantity which transforms as a world scalar under the Lorentz group, for instance, in the Standard Model, the vacuum expectation value $\langle \Phi \rangle$ of the Higgs field. However, this does not necessarily imply that the vacuum state itself has to be *Lorentz invariant*. Namely, Lorentz transformation operators

U', U'', \dots could transform non trivially the reference vacuum state ¹ $|\Psi^{(0)}\rangle$ (appropriate to an observer at rest in Σ) into $|\Psi'\rangle, |\Psi''\rangle, \dots$ (appropriate to moving observers S', S'', \dots) and still, for any Lorentz-invariant operator G , one would find

$$\langle G \rangle_{\Psi^{(0)}} = \langle G \rangle_{\Psi'} = \langle G \rangle_{\Psi''} = \dots \quad (3)$$

For the convenience of the reader, we will report in the Appendix the main ingredients to understand the origin of the problem (see also [6]). Here, in this Introduction, we will only limit ourselves to the general conclusion: imposing that only scalar fields can acquire a non-vanishing vacuum expectation value does *not* guarantee that the vacuum state itself is Lorentz invariant.

This preliminary discussion is important because, on this basis, the mentioned global frame could also reflect a vacuum structure with some degree of substantiality and thus characterize non-trivially the form of relativity which is physically realized in nature. In other words, as in the original Lorentzian formulation, Lorentz transformations could still be exact to connect two observers in uniform translational motion but there would be a preferred reference frame. In this case, the isotropy of the CMB radiation would just *indicate* the existence of such a global frame that we could decide to call the “ether”, but the cosmic radiation itself would *not* coincide with this type of ether. Ultimate implications are far reaching. Think for instance of the possibility, with a preferred frame, to reconcile faster-than-light signals with causality [8] and thus provide a very different view of the apparent non-local aspects of the quantum theory [9] ².

Therefore, once the answer to our basic question cannot be found with theoretical arguments only, one should look at experiments, in particular at the so called “ether-drift” experiments where one tries to measure a small difference of the velocity of light in different directions and, eventually, to find a definite correlation with the direct CMB observations in space. At present, the general consensus is that no physical ether drift has ever been detected. This standard view considers all available data (from Michelson-Morley until the modern interference experiments with optical resonators) as a long sequence of null results, i.e. typical instrumental effects obtained in measurements with better and better systematics.

However, by accepting the idea of a preferred reference frame, and if the velocity of light propagating in the various interferometers is not *exactly* the same parameter c of Lorentz transformations, nothing would really prevent to observe an ether drift. For this reason, it is natural to enquire to which extent the experiments performed so far have really given null results. By changing the theoretical model, small residual effects which apparently represent

¹ We ignore here the problem of vacuum degeneracy by assuming that any overlapping among equivalent vacua vanishes in the infinite-volume limit of quantum field theory (see e.g. S. Weinberg, *The Quantum Theory of Fields*, Cambridge University press, Vol.II, pp. 163-167).

²The importance of establishing a link between CMB and ether-drift experiments is better illustrated by quoting from ref.[10] where Hardy discusses the implications of the typical non-locality of the quantum theory: “Thus, Nonlocality is most naturally incorporated into a theory in which there is a special frame of reference. One possible candidate for this special frame of reference is the one in which the cosmic background radiation is isotropic. However, other than the fact that a realistic interpretation of quantum mechanics requires a preferred frame and the cosmic background radiation provides us with one, there is no readily apparent reason why the two should be linked”.

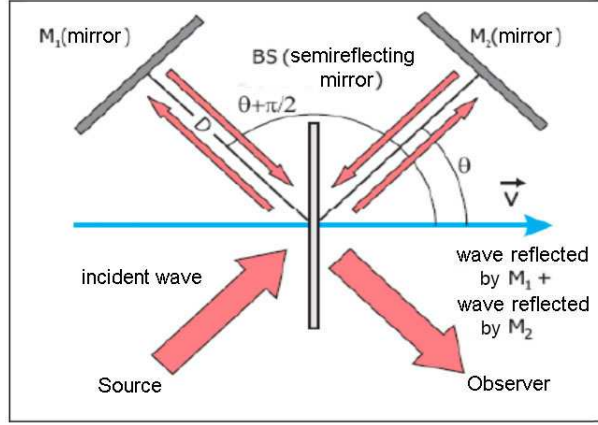


Figure 1: *The typical scheme of Michelson's interferometer.*

spurious instrumental artifacts could acquire a definite physical meaning with substantial implications for both physics and the history of science.

1.2 Basics of the ether-drift experiments

To introduce the argument, it is necessary to recall the basic ingredients of the ether-drift experiments starting from the original 1887 Michelson-Morley experiment [11]. Nowadays, this fundamental experiment and its early repetitions performed at the turn of 19th and 20th centuries (by Miller [12], Kennedy [13], Illingworth [14], Joos [15]...) are considered as a venerable, well understood historical chapter for which, at least from a physical point of view, there is nothing more to refine or clarify. All emphasis is now on the modern versions of these experiments, with lasers stabilized by optical cavities, see e.g. [16] for a review. These modern experiments adopt a very different technology but, in the end, have exactly the same scope: searching for the possible existence of a preferred reference frame through an anisotropy of the two-way velocity of light $\bar{c}_\gamma(\theta)$. This is the only one that can be measured unambiguously and is defined in terms of the one-way velocity $c_\gamma(\theta)$ as

$$\bar{c}_\gamma(\theta) = \frac{2 c_\gamma(\theta) c_\gamma(\pi + \theta)}{c_\gamma(\theta) + c_\gamma(\pi + \theta)} \quad (4)$$

Here θ represents the angle between the direction of light propagation and the earth velocity with respect to the hypothetical preferred frame Σ . By introducing the anisotropy

$$\Delta\bar{c}_\theta = \bar{c}_\gamma(\pi/2 + \theta) - \bar{c}_\gamma(\theta)$$

there is a simple relation with the time difference $\Delta t(\theta)$ for light propagation back and forth along perpendicular rods of length D . In fact, by assuming the validity of Lorentz transformations, the length of a rod does not depend on its orientation, in the S' frame where it is at rest, and one finds

$$\Delta t(\theta) = \frac{2D}{\bar{c}_\gamma(\theta)} - \frac{2D}{\bar{c}_\gamma(\pi/2 + \theta)} \sim \frac{2D}{c} \frac{\Delta\bar{c}_\theta}{c} \quad (5)$$

(where, in the last relation, we have assumed that light propagates in a medium of refractive index $\mathcal{N} = 1 + \epsilon$, with $\epsilon \ll 1$). This gives directly the fringe patterns (λ is the light wavelength)

$$\frac{\Delta\lambda(\theta)}{\lambda} \sim \frac{2D}{\lambda} \frac{\Delta\bar{c}_\theta}{c} \quad (6)$$

which were measured with Michelson interferometers in classical ether-drift experiments, see Fig.1.

In modern experiments, on the other hand, a possible anisotropy of $\bar{c}_\gamma(\theta)$ would show up through the relative frequency shift, i.e. the beat signal, $\Delta\nu(\theta)$ of two orthogonal optical resonators. Their frequency

$$\nu(\theta) = \frac{\bar{c}_\gamma(\theta)m}{2L} \quad (7)$$

is proportional to the two-way velocity of light within the resonator through an integer number m , which fixes the cavity mode, and the length of the cavity L as measured in the laboratory S' frame. Therefore, once the length of a cavity in its rest frame does not depend on its orientation, one finds

$$\frac{\Delta\nu(\theta)}{\nu_0} \sim \frac{\Delta\bar{c}_\theta}{c} \quad (8)$$

where ν_0 is the reference frequency of the two resonators.

Within this basic scheme, let us now see how experimental results are presented, in particular in the recent work of Nagel et al. [17]. Their measurements amount to an *average* fractional anisotropy $|\langle \frac{\Delta\bar{c}_\theta}{c} \rangle| \lesssim 10^{-18}$. With this new result, by looking at their Fig.1 where all ether-drift experiments are reported, one gets the impression of a steady, substantial improvement over the original 1887 Michelson-Morley result $\frac{|\Delta\bar{c}_\theta|}{c} = \mathcal{O}(10^{-10})$. All together, their plot supports the mentioned view of a series of null results with better and better systematics.

Still, over the years, greatest experts [18, 12] have seriously questioned the traditional null interpretation of the very early measurements. In their opinion, the small residuals should not be neglected. Therefore one may wonder if, indeed, this first impression is correct. For instance, the various measurements were performed in different conditions, i.e. with light propagating in gaseous media (as in [11, 12, 13, 14, 15]) or in a high vacuum (as in [19, 20, 21, 22, 23]) or inside dielectrics with a large refractive index (as in [24, 17]) and there could be physical reasons which prevent a straightforward comparison. In this case, the difference between old experiments (in air or gaseous helium) and modern experiments (in vacuum or solid dielectrics) might not depend on the technological progress only but also on the different media that were tested.

With this perspective, let us re-consider Maxwell's classical calculation [25] of light anisotropy with a preferred frame which was at the base of the ether-drift experiments. We know that his original estimate, namely $\frac{|\Delta\bar{c}_\theta|}{c} \sim \beta^2$, is wrong. However, even by assuming the exact validity of Lorentz transformations, Maxwell's problem still makes sense. The point is that, for a refractive index $\mathcal{N} = 1 + \epsilon$, in the $\epsilon \rightarrow 0$ limit where the velocity of light tends to coincide with the basic parameter c entering Lorentz transformations, simple symmetry arguments suggest that a possible non-zero result has the form $\frac{|\Delta\bar{c}_\theta|}{c} \sim \epsilon\beta^2$. From this relation and by assuming the typical value $v \sim 370$ km/s for the earth cosmic motion, for air

at room temperature and atmospheric pressure where the refractivity is $\mathcal{N} - 1 \sim 2.8 \cdot 10^{-4}$ and for gaseous helium at room temperature and atmospheric pressure where the refractivity is $\mathcal{N} - 1 \sim 3.3 \cdot 10^{-5}$, one gets anisotropy values, respectively $\frac{|\Delta\bar{c}_\theta|}{c} = \mathcal{O}(10^{-10})$ and $\frac{|\Delta\bar{c}_\theta|}{c} = \mathcal{O}(10^{-11})$, which are much smaller than the classical prediction $\frac{|\Delta\bar{c}_\theta|}{c} \sim 10^{-8}$ (for the traditional orbital value $v = 30$ km/s) and consistent with the actual observations.

At the same time, symmetry arguments give often a successful description of phenomena independently of the particular physical mechanisms. As such, this view does not necessarily contradict the standard interpretation of the residuals as thermal disturbances. Indeed, as pointed out by Kennedy [13], also these disturbances become smaller and smaller for $\epsilon \rightarrow 0$. For this reason, periodic temperature variations of $1 \div 2$ millikelvin in the air of the optical arms, were considered by Shankland et al. [26], Kennedy (see p. 175 of ref.[26]) and Joos [27] to explain away Miller's observations, but were never fully understood. As such, these thermal effects might have a *non-local* origin somehow associated with an earth velocity v , e.g. our motion within the CMB. Finding such an explanation, where symmetry arguments, on the one hand, motivate and, on the other hand, find justification in underlying physical mechanisms, would greatly increase our understanding. We will return to this crucial point in the following.

1.3 Nature of the vacuum and time dependence of the data

After the magnitude of the signal, the other important aspect of the ether-drift experiments concerns the time dependence of the data. Traditionally, it has always been assumed that, for short-time observations of a few days, where there are no sizeable changes in the earth orbital velocity, the time dependence of a genuine physical signal should reproduce the slow and regular modulations induced by the earth rotation. The data instead, for both classical and modern experiments, have always shown a very irregular behavior. As a consequence, all statistical averages are much smaller than the instantaneous values. For instance, compare the average anisotropy $|\langle \frac{\Delta\bar{c}_\theta}{c} \rangle| \lesssim 10^{-18}$ obtained in ref.[17] by combining a large number of observations with its typical, *instantaneous* determination $\frac{|\Delta\bar{c}_\theta|}{c} \lesssim 10^{-15}$ shown in their Fig.3 b. This difference, between single measurements and statistical averages, has always represented a strong argument to interpret the data as mere instrumental artifacts.

However, again, could there be an alternative interpretative scheme? In other words, could a definite *instantaneous* value $\frac{\Delta\bar{c}_\theta}{c} \neq 0$ coexist with its vanishing statistical average $|\langle \frac{\Delta\bar{c}_\theta}{c} \rangle|$? This possibility was considered in refs.[28, 29] by modeling the physical vacuum as a fundamental stochastic medium, somehow similar to an underlying turbulent fluid.

To understand the motivations, let us observe that it is the nature of the physical vacuum to determine the relation between the macroscopic earth motion and the microscopic optical measurements in a laboratory. Light propagation (e.g. inside an optical cavity) takes place in this substratum which is dragged along the earth motion but, so to speak, is not rigidly connected with the solid parts of the apparatus as fixed in the laboratory. Therefore, if one would try to characterize its local state of motion, say $v_\mu(t)$, this does not necessarily coincide with the projection of the global earth motion, say $\tilde{v}_\mu(t)$, at the observation site. The latter is a smooth function while the former, $v_\mu(t)$, in principle is unknown. By comparing with

the motion of a body in a fluid, the equality $v_\mu(t) = \tilde{v}_\mu(t)$ amounts to assume a form of regular, laminar flow where global and local velocity fields coincide. Instead, in a turbulent fluid large-scale and small-scale flows would only be *indirectly* related.

The simplest explanation for the turbulent-fluid analogy is the intuitive representation of the vacuum as a fluid with vanishing viscosity. Then, in the framework of the Navier-Stokes equation, a laminar flow is by no means obvious due to the subtlety of the zero-viscosity (or infinite Reynolds number) limit, see for instance the discussion given by Feynman in Sect. 41.5, Vol.II of his Lectures [30]. The reason is that the velocity field of such a hypothetical fluid cannot be a differentiable function [31] and one should think, instead, in terms of continuous, nowhere differentiable functions, similar to ideal Brownian paths [32]. This gives the idea of the vacuum as a fundamental stochastic medium consistently with some basic foundational aspects of *both* quantum physics and relativity ³.

On this basis, in refs.[28, 29] the signal was characterized as in the simulations of turbulent flows. Namely, the local $v_\mu(t)$ exhibits random fluctuations while the global $\tilde{v}_\mu(t)$ determines its typical boundaries. Then, if turbulence becomes homogeneous and isotropic at small scales, as it is generally accepted in the limit of zero viscosity, the direction of the local drift becomes a completely random quantity which has no definite limit by combining a large number of observations. Since vectorial quantities have vanishing statistical averages, one should thus analyze the data in phase and amplitude (which give respectively the instantaneous direction and magnitude of the local drift) and concentrate on the latter which is a positive-definite quantity and remains non-zero under any averaging procedure. In this alternative picture of the ether drift, a non-vanishing amplitude (i.e. definitely larger than the experimental resolution) becomes the signature to separate an irregular, but genuine, physical signal from spurious instrumental noise. If non-zero, its time modulations can then be compared with models of the earth cosmic motion.

1.4 Comparing experiments in gases, vacuum and solid dielectrics

After these preliminaries, a definite quantitative framework to analyze the experiments will be presented in Sects.2 and 3. Our scheme can be considered a modern version of the original Maxwell calculation. It applies to the infinitesimal region of refractive index $\mathcal{N} = 1 + \epsilon$ and, within the analogy of a turbulent flow, takes into account random fluctuations of the local

³This picture was first proposed in the old ether theory at the end of XIX Century [33]. In this original derivation, the Lorentz covariance of Maxwell equations was not postulated from scratch but was emerging from an underlying physical system whose constituents obey classical mechanics. More recently, the turbulent-ether model has been re-formulated by Troshkin [34] (see also [35] and [36]) in the framework of the Navier-Stokes equation and by Saul [37] by starting from Boltzmann's transport equation. As another example, the same picture of the physical vacuum (or ether) as a turbulent fluid was Nelson's [38] starting point. In particular, the zero-viscosity limit gave him the motivation to expect that "the Brownian motion in the ether will not be smooth" and, therefore, to conceive the particular form of kinematics which is at the base of his stochastic derivation of the Schrödinger equation. A qualitatively similar picture is also obtained by representing relativistic particle propagation from the superposition, at very short time scales, of non-relativistic particle paths with different Newtonian mass [39]. In this formulation, particles randomly propagate (in the sense of Brownian motion) in an underlying granular medium which replaces the trivial empty vacuum [40]. For more details, see [29].

drift around the average earth motion. As a matter of fact, see Sect.4, when this scheme is used to describe the small residuals of the classical ether-drift experiments in gaseous systems, it yields typical earth velocities which are consistent with the value of 370 km/s obtained from the CMB observations. Confirming (or excluding) this alternative interpretation will thus require a new series of dedicated experiments. The essential aspect is that the optical resonators, which are coupled to the lasers, should be filled by gaseous media. In this way, one could reproduce the experimental conditions of those early measurements with today's much greater accuracy. Such experiments would be along the lines of ref.[41] where just the use of optical cavities filled with different forms of matter was considered as a useful complementary tool to study deviations from exact Lorentz invariance.

Waiting for this new series of experimental tests, however, we have tried to check the same scheme in modern vacuum experiments. The point is that for the *physical* vacuum the ideal equality $\mathcal{N}_v = 1$ might not be exact. For instance, it was proposed in [42] that, if the curvature observed in a gravitational field is an emergent phenomenon from a fundamentally flat space-time, there should be a small vacuum refractivity $\epsilon_v = \mathcal{N}_v - 1 \sim 10^{-9}$. This would take into account the difference which exists, in this case, between an apparatus in an ideal freely falling frame and an apparatus placed on the earth surface. The basic argument will be repeated in Sect.5 with many additional details not reported in [42]. The existence of a preferred frame would then imply in our picture a definite, instantaneous $\frac{|\Delta\bar{c}_\theta|}{c} \sim \epsilon_v\beta^2 \sim 10^{-15}$ which coexists with much smaller statistical averages $|\langle\frac{\Delta\bar{c}_\theta}{c}\rangle| \ll 10^{-15}$. In Sect. 6, this expectation will be shown to be consistent with the most recent room temperature and cryogenic vacuum experiments.

Then, in Sect.7, we will re-consider from scratch the temperature dependence of the refractivity in gaseous media. This calculation shows that the light anisotropy $\frac{|\Delta\bar{c}_\theta|}{c} \sim \epsilon\beta^2$ observed in gases could also be interpreted as a thermal effect due to a tiny, non-local temperature gradient of a fraction of millikelvin. This is found in all classical experiments and might be related to the CMB temperature dipole of ± 3 mK or also reflect the fundamental energy flow expected in a Lorentz-non-invariant vacuum. Whatever its ultimate origin, the interesting point is that this thermal interpretation provides a dynamical basis for the *enhancement* found in weakly bound gaseous matter (i.e. the observed magnitudes $\frac{|\Delta\bar{c}_\theta|}{c} = \mathcal{O}(10^{-10})$ and $\frac{|\Delta\bar{c}_\theta|}{c} = \mathcal{O}(10^{-11})$ vs. the much smaller vacuum value $\frac{|\Delta\bar{c}_\theta|}{c} \lesssim 10^{-15}$) and, at the same time, can help to understand the differences and the analogies with experiments in strongly bound solid dielectrics where the refractivity is $\mathcal{O}(1)$ but again an instantaneous value $\frac{|\Delta\bar{c}_\theta|}{c} \lesssim 10^{-15}$ (as in the vacuum case) is presently observed.

We emphasize that, due to this alternative view of the ether-drift experiments in gases, precise measurements where optical cavities are maintained in an extremely high vacuum, both at room temperature and in the cryogenic regime, become essential to exclude a purely thermal interpretations of light anisotropy, as for instance ultimately associated with the CMB temperature dipole. In fact, once any residual gaseous matter is totally negligible, the definite persistence in vacuum of the 10^{-15} instantaneous signal would support the more radical idea of a genuine preferred frame for relativity.

In the end, Sect.8 will contain a summary and our conclusions.

2. A modern version of Maxwell's calculation

To start with, let us introduce the parameter ϵ defined by the relation $\epsilon = (\mathcal{N} - 1) \ll 1$, \mathcal{N} being the refractive index of the medium where light propagates. For instance, the medium (e.g. a gas) could fill an optical cavity at rest in a frame S' which moves with uniform velocity v with respect to the hypothetical Σ . Now, by assuming i) that the velocity of light is exactly isotropic when $S' \equiv \Sigma$ and ii) the validity of Lorentz transformations, then any anisotropy in S' should vanish identically either for $v = 0$ or for the ideal vacuum case $\mathcal{N} = 1$ when the velocity of light c_γ coincides with the basic parameter c entering Lorentz transformations⁴. Thus, one can expand in powers of the two small parameters ϵ and $\beta = v/c$. By taking into account that, by its very definition, the two-way velocity $\bar{c}_\gamma(\theta)$ is invariant under the replacement $\beta \rightarrow -\beta$ and that, for any fixed β , is also invariant under the replacement $\theta \rightarrow \pi + \theta$, to lowest non-trivial level $\mathcal{O}(\epsilon\beta^2)$, one finds the general expression [28, 6]

$$\bar{c}_\gamma(\theta) \sim \frac{c}{\mathcal{N}} \left[1 - \epsilon \beta^2 \sum_{n=0}^{\infty} \zeta_{2n} P_{2n}(\cos \theta) \right] \quad (9)$$

Here, to take into account invariance under $\theta \rightarrow \pi + \theta$, the angular dependence has been given as an infinite expansion of even-order Legendre polynomials with arbitrary coefficients $\zeta_{2n} = \mathcal{O}(1)$. In Einstein's special relativity, where there is no preferred reference frame, these ζ_{2n} coefficients should vanish identically. In a ‘‘Lorentzian’’ approach, on the other hand, there is no reason why they should vanish *a priori*.

By leaving out the first few ζ 's as free parameters in the fits, Eq.(9) can already represent a viable form to compare with experiments. Still, one can further sharpen the predictions by exploiting one more derivation of the $\epsilon \rightarrow 0$ limit with a preferred frame. This other argument is based on the effective space-time metric $g^{\mu\nu} = g^{\mu\nu}(\mathcal{N})$ which, through the relation $g^{\mu\nu} p_\mu p_\nu = 0$, describes light propagation in a medium of refractive index \mathcal{N} , see e.g. [44] and references quoted therein. For the quantum theory, a derivation of this metric from first principles was given by Jauch and Watson [45] who worked out the quantization of the electromagnetic field in a dielectric. They noticed that the procedure introduces unavoidably a preferred reference frame, the one where the photon energy spectrum does not depend on the direction of propagation, and which is ‘‘usually taken as the system for which the medium is at rest’’. However, such an identification reflects the point of view of special relativity with no preferred frame. Instead, one can adapt their results to the case where the angle-independence of the photon energy is only valid when both medium and observer are at rest in some particular frame Σ .

With this premise, let us consider two identical optical cavities, namely cavity 1, at rest in Σ , and cavity 2, at rest in S' , and denote by $\pi_\mu \equiv (\frac{E_\pi}{c}, \boldsymbol{\pi})$ the light 4-momentum for Σ in his cavity 1 and by $p_\mu \equiv (\frac{E_p}{c}, \mathbf{p})$ the corresponding light 4-momentum for S' in his cavity 2. Let us also denote by $g^{\mu\nu}$ the space-time metric that S' uses in the relation $g^{\mu\nu} p_\mu p_\nu = 0$ and

⁴Actually, Guerra and De Abreu have shown [43] that the null result of a Michelson-Morley experiment in an ideal vacuum can also be deduced without using Lorentz transformations, but only from general assumptions on the choice of the admissible clocks.

by

$$\gamma^{\mu\nu} = \text{diag}(\mathcal{N}^2, -1, -1, -1) \quad (10)$$

the metric used by Σ in the relation $\gamma^{\mu\nu}\pi_\mu\pi_\nu = 0$ and which gives an isotropic velocity $c_\gamma = E_\pi/|\pi| = \frac{c}{\mathcal{N}}$. Notice that, in this framework, special relativity is included as a particular case where there is no observable difference between Σ and S' and the two frames are placed on the same footing.

Let us first consider the ideal vacuum limit $\mathcal{N} = 1$. Here, the frame independence of the velocity of light requires to impose

$$g^{\mu\nu}(\mathcal{N} = 1) = \gamma^{\mu\nu}(\mathcal{N} = 1) = \eta^{\mu\nu} \quad (11)$$

where $\eta^{\mu\nu}$ is the Minkowski tensor. This standard equality amounts to introduce a transformation matrix, say A_ν^μ , such that

$$g^{\mu\nu} = A_\rho^\mu A_\sigma^\nu \eta^{\rho\sigma} = \eta^{\mu\nu} \quad (12)$$

This relation is strictly valid for $\mathcal{N} = 1$. However, by continuity, one is driven to conclude that an analogous relation between $g^{\mu\nu}$ and $\gamma^{\mu\nu}$ should also hold in the $\epsilon \rightarrow 0$ limit. The only subtlety is that relation (12) does not fix uniquely A_ν^μ . In fact, one can either choose the identity matrix, i.e. $A_\nu^\mu = \delta_\nu^\mu$, or a Lorentz transformation, i.e. $A_\nu^\mu = \Lambda_\nu^\mu$. Since for any finite v these two matrices cannot be related by an infinitesimal transformation, it follows that A_ν^μ is a two-valued function in the $\epsilon \rightarrow 0$ limit.

Therefore, in principle, there are two solutions. Namely, if A_ν^μ is the identity matrix, we expect a first solution

$$[g^{\mu\nu}(\mathcal{N})]_1 = \gamma^{\mu\nu} \sim \eta^{\mu\nu} + 2\epsilon\delta_0^\mu\delta_0^\nu \quad (13)$$

while, if A_ν^μ is a Lorentz transformation, we expect the other solution

$$[g^{\mu\nu}(\mathcal{N})]_2 = \Lambda_\rho^\mu \Lambda_\sigma^\nu \gamma^{\rho\sigma} \sim \eta^{\mu\nu} + 2\epsilon v^\mu v^\nu \quad (14)$$

v^μ being the dimensionless S' 4-velocity, $v^\mu \equiv (v^0, \mathbf{v}/c)$ with $v_\mu v^\mu = 1$.

Notice that with the former choice, implicitly adopted in special relativity to preserve isotropy in all reference systems also for $\mathcal{N} \neq 1$, one is introducing a discontinuity in the transformation matrix for any $\epsilon \neq 0$. Indeed, the whole emphasis on Lorentz transformations depends on enforcing Eq.(12) for $A_\nu^\mu = \Lambda_\nu^\mu$ so that $\Lambda^{\mu\sigma}\Lambda_\sigma^\nu = \eta^{\mu\nu}$ and the Minkowski metric applies to all equivalent frames.

On the other hand, with the latter solution, by replacing in the relation $p_\mu p_\nu g^{\mu\nu} = 0$, the photon energy now depends on the direction of propagation. Then, by defining the light velocity $c_\gamma(\theta)$ from the ratio $E_p/|\mathbf{p}|$, one finds [28, 6]

$$c_\gamma(\theta) \sim \frac{c}{\mathcal{N}} [1 - 2\epsilon\beta \cos\theta - \epsilon\beta^2(2 - \sin^2\theta)] \quad (15)$$

and a two-way velocity

$$\bar{c}_\gamma(\theta) = \frac{2 c_\gamma(\theta)c_\gamma(\pi + \theta)}{c_\gamma(\theta) + c_\gamma(\pi + \theta)} \sim (c/\mathcal{N}) [1 - \epsilon\beta^2 (2 - \sin^2\theta)] \quad (16)$$

where θ is the angle between \mathbf{v} and \mathbf{p} (as defined in the S' frame).

Eq.(16) corresponds to setting in Eq.(9) $\zeta_0 = 4/3$, $\zeta_2 = 2/3$ and all $\zeta_{2n} = 0$ for $n > 1$ and can be considered a modern version of Maxwell's original calculation. It represents a definite, alternative model for the interpretation of experiments performed close to the ideal vacuum limit $\epsilon = 0$, such as in gaseous systems, and will be adopted in the following.

A conceptual detail concerns the relation of the gas refractive index \mathcal{N} , as introduced in Eq.(10), to the experimental quantity \mathcal{N}_{exp} which is extracted from measurements of the two-way velocity in the earth laboratory. By introducing a θ -dependent refractive index through the relation

$$\bar{c}_\gamma(\theta) \equiv \frac{c}{\mathcal{N}(\theta)} \quad (17)$$

one should thus define the experimental value by an angular average of Eq.(16), i.e.

$$\frac{c}{\mathcal{N}_{\text{exp}}} \equiv \langle \frac{c}{\mathcal{N}(\theta)} \rangle_\theta = \frac{c}{\mathcal{N}} \left[1 - \frac{3}{2}(\mathcal{N} - 1)\beta^2 \right] \quad (18)$$

From this relation, one can determine in principle the unknown value $\mathcal{N} \equiv \mathcal{N}(\Sigma)$ (as if the container of the gas were at rest in Σ), in terms of the experimentally known quantity $\mathcal{N}_{\text{exp}} \equiv \mathcal{N}(\text{earth})$ and of v . For instance, for air the most precise determinations are at the level 10^{-7} , say $\mathcal{N}_{\text{exp}} = 1.0002924..$ for light of 589 nm, at 0 °C and atmospheric pressure. In practice, for the standard velocity values involved in most cosmic motions, say $v \sim 300$ km/s, the difference between $\mathcal{N}(\Sigma)$ and $\mathcal{N}(\text{earth})$ is below 10^{-9} and thus completely negligible. The same holds true for the other gaseous systems (say nitrogen, carbon dioxide, helium,..) for which the present experimental accuracy in the refractive index is, at best, at the level 10^{-7} . Finally, the isotropic two-way speed of light is better determined in the low-pressure limit where $(\mathcal{N} - 1) \rightarrow 0$. In the same limit, for any given value of v , the approximation $\mathcal{N}(\Sigma) = \mathcal{N}(\text{earth})$ becomes better and better.

From Eq.(16) we obtain a fractional anisotropy

$$\frac{\Delta \bar{c}_\theta}{c} = \frac{\bar{c}_\gamma(\pi/2 + \theta) - \bar{c}_\gamma(\theta)}{c} \sim \epsilon \frac{v^2}{c^2} \cos 2(\theta - \theta_0) \quad (19)$$

Here v and θ_0 are respectively the magnitude and the direction of the drift in the plane of the interferometer so that, from Eq.(6), one finds directly the fringe pattern

$$\frac{\Delta \lambda(\theta)}{\lambda} = \frac{2D}{\lambda} \frac{\Delta \bar{c}_\theta}{c} \sim 2\epsilon \frac{D}{\lambda} \frac{v^2}{c^2} \cos 2(\theta - \theta_0) \quad (20)$$

In this scheme, the ether drift is a second-harmonic effect, i.e. periodic in the range $[0, \pi]$, as in the classical theory (see e.g. [46] for a simple derivation). Only its amplitude

$$A_2 = 2\epsilon \frac{D}{\lambda} \frac{v^2}{c^2} \quad (21)$$

is suppressed by the very small factor 2ϵ with respect to the classical prediction

$$A_2^{\text{class}} = \frac{D}{\lambda} \frac{v^2}{c^2} \quad (22)$$

Thus one can re-absorb all effects into a much smaller *observable* velocity

$$v_{\text{obs}}^2 \sim 2\epsilon v^2 \quad (23)$$

which depends on the gas refractive index and is the one traditionally reported in the classical analysis of the data.

However, as anticipated in the Introduction, for a proper comparison with experiments a change of perspective is needed in the physical description of the ether-drift phenomenon. In the following section, we will illustrate a simple stochastic model that we propose for the analysis of the data.

3. A stochastic form of ether-drift

To make explicit the time dependence of the signal let us re-write Eq.(19) as

$$\frac{\Delta \bar{c}_\theta(t)}{c} \sim \epsilon \frac{v^2(t)}{c^2} \cos 2(\theta - \theta_0(t)) \quad (24)$$

where $v(t)$ and $\theta_0(t)$ indicate respectively the instantaneous magnitude and direction of the drift in the plane of the interferometer. This can also be re-written as

$$\frac{\Delta \bar{c}_\theta(t)}{c} \sim 2S(t) \sin 2\theta + 2C(t) \cos 2\theta \quad (25)$$

with

$$2C(t) = \epsilon \frac{v_x^2(t) - v_y^2(t)}{c^2} \quad 2S(t) = \epsilon \frac{2v_x(t)v_y(t)}{c^2} \quad (26)$$

and $v_x(t) = v(t) \cos \theta_0(t)$, $v_y(t) = v(t) \sin \theta_0(t)$

As anticipated in the Introduction, the standard assumption to analyze the data is based on the idea of smooth, regular modulations of the signal associated with a cosmic earth velocity. In general, this is characterized by a magnitude V , a right ascension α and an angular declination γ . These parameters can be considered constant for short-time observations of a few days where there are no appreciable changes due to the earth orbital velocity around the sun. In this framework, where the only time dependence is due to the earth rotation, the traditional identifications are $v(t) \equiv \tilde{v}(t)$ and $\theta_0(t) \equiv \tilde{\theta}_0(t)$ where $\tilde{v}(t)$ and $\tilde{\theta}_0(t)$ derive from the simple application of spherical trigonometry [47]

$$\cos z(t) = \sin \gamma \sin \phi + \cos \gamma \cos \phi \cos(\tau - \alpha) \quad (27)$$

$$\tilde{v}(t) = V \sin z(t) \quad (28)$$

$$\tilde{v}_x(t) = \tilde{v}(t) \cos \tilde{\theta}_0(t) = V [\sin \gamma \cos \phi - \cos \gamma \sin \phi \cos(\tau - \alpha)] \quad (29)$$

$$\tilde{v}_y(t) = \tilde{v}(t) \sin \tilde{\theta}_0(t) = V \cos \gamma \sin(\tau - \alpha) \quad (30)$$

Here $z = z(t)$ is the zenithal distance of \mathbf{V} , ϕ is the latitude of the laboratory, $\tau = \omega_{\text{sid}} t$ is the sidereal time of the observation in degrees ($\omega_{\text{sid}} \sim \frac{2\pi}{23^h 56'}$) and the angle θ_0 is counted conventionally from North through East so that North is $\theta_0 = 0$ and East is $\theta_0 = 90^\circ$.

With the identifications $v(t) \equiv \tilde{v}(t)$ and $\theta_0(t) \equiv \tilde{\theta}_0(t)$, one thus arrives to the simple Fourier decomposition

$$S(t) \equiv \tilde{S}(t) = S_0 + S_{s1} \sin \tau + S_{c1} \cos \tau + S_{s2} \sin(2\tau) + S_{c2} \cos(2\tau) \quad (31)$$

$$C(t) \equiv \tilde{C}(t) = C_0 + C_{s1} \sin \tau + C_{c1} \cos \tau + C_{s2} \sin(2\tau) + C_{c2} \cos(2\tau) \quad (32)$$

where the C_k and S_k Fourier coefficients depend on the three parameters (V, α, γ) (see [16]) and, to very good approximation, should be time-independent for short-time observations.

However, identifying the instantaneous quantities $v_x(t)$ and $v_y(t)$, with their counterparts $\tilde{v}_x(t)$ and $\tilde{v}_y(t)$ is equivalent to assume a form of regular, laminar flow where global and local velocity fields coincide. Instead, as anticipated in the Introduction, one may consider the alternative model of a turbulent flow where the two sets of quantities are only *indirectly* related. This picture is motivated by the idea of the vacuum as a stochastic medium for which the local velocity field becomes non-differentiable and the ordinary formulation in terms of differential equations breaks down [31, 32]. Thus, one has to adopt some other description, for instance a formulation in terms of random Fourier series [31, 48, 49]. In this other approach, the parameters of the macroscopic motion are only used to fix the typical boundaries for a microscopic velocity field which has an intrinsic non-deterministic nature.

The simplest model, adopted in refs.[28, 29], corresponds to a turbulence which, at small scales, appears homogeneous and isotropic ⁵. The analysis of Sect.2, can then be embodied in an effective space-time metric for light propagation

$$\hat{g}^{\mu\nu}(t) \sim \eta^{\mu\nu} + 2\epsilon \hat{v}^\mu(t) \hat{v}^\nu(t) \quad (33)$$

where $\hat{v}^\mu(t)$ is a random 4-velocity field which describes the drift and whose boundaries depend on a smooth field $\tilde{v}^\mu(t)$ determined by the average earth motion. If this corresponds to the actual physical situation, it is easy to see why a genuine stochastic signal can become consistent with average values $(C_k)^{\text{avg}} = (S_k)^{\text{avg}} = 0$ obtained by fitting the data with Eqs.(31) and (32).

Our intention is to simulate the two components of the velocity in the x-y plane, at a given fixed location in the laboratory, to reproduce the $S(t)$ and $C(t)$ functions Eq.(26). For a homogeneous turbulence, one finds the general expressions

$$\hat{v}_x(t) = \sum_{n=1}^{\infty} [x_n(1) \cos \omega_n t + x_n(2) \sin \omega_n t] \quad (34)$$

$$\hat{v}_y(t) = \sum_{n=1}^{\infty} [y_n(1) \cos \omega_n t + y_n(2) \sin \omega_n t] \quad (35)$$

where $\omega_n = 2n\pi/T$, T being a time scale which represents a common period of all stochastic components. For numerical simulations, the typical value $T = T_{\text{day}} = 24$ hours was adopted [28, 29]. However, it was also checked with a few runs that the statistical distributions of

⁵This picture reflects the basic Kolmogorov theory [50] of a fluid with vanishingly small viscosity.

the various quantities do not change substantially by varying T in the rather wide range $0.1 T_{\text{day}} \leq T \leq 10 T_{\text{day}}$.

The coefficients $x_n(i = 1, 2)$ and $y_n(i = 1, 2)$ are random variables with zero mean and have the physical dimension of a velocity. In general, we can denote by $[-d_x(t), d_x(t)]$ the range for $x_n(i = 1, 2)$ and by $[-d_y(t), d_y(t)]$ the corresponding range for $y_n(i = 1, 2)$. Statistical isotropy would require to impose $d_x(t) = d_y(t)$. However, to illustrate the more general case, let us first consider $d_x(t) \neq d_y(t)$. In terms of these boundaries, the only non-vanishing (quadratic) statistical averages are

$$\langle x_n^2(i = 1, 2) \rangle_{\text{stat}} = \frac{d_x^2(t)}{3 n^{2\eta}} \quad \langle y_n^2(i = 1, 2) \rangle_{\text{stat}} = \frac{d_y^2(t)}{3 n^{2\eta}} \quad (36)$$

in a uniform-probability model within the intervals $[-d_x(t), d_x(t)]$ and $[-d_y(t), d_y(t)]$. Here, the exponent η controls the power spectrum of the fluctuating components. For numerical simulations, between the two values $\eta = 5/6$ and $\eta = 1$ reported in ref.[49], we have adopted $\eta = 1$ which corresponds to the Lagrangian description where the point of measurement is a wandering material point in the fluid.

Finally, the connection with the earth cosmic motion is obtained by identifying $d_x(t) = \tilde{v}_x(t)$ and $d_y(t) = \tilde{v}_y(t)$ as given in Eqs. (27)–(30). In this case, it is natural to adopt the set $V = 370$ km/s, $\alpha = 168$ degrees, $\gamma = -7$ degrees, which describes the average earth motion with respect to the CMB.

If, however, we require statistical isotropy, the relation

$$\tilde{v}_x^2(t) + \tilde{v}_y^2(t) = \tilde{v}^2(t) \quad (37)$$

requires the identification ⁶

$$d_x(t) = d_y(t) = \frac{\tilde{v}(t)}{\sqrt{2}} \quad (38)$$

For such isotropic model, by combining Eqs.(34)–(38) and in the limit of an infinite statistics, one gets

$$\begin{aligned} \langle \hat{v}_x^2(t) \rangle_{\text{stat}} = \langle \hat{v}_y^2(t) \rangle_{\text{stat}} &= \frac{\tilde{v}^2(t)}{2} \frac{1}{3} \sum_{n=1}^{\infty} \frac{1}{n^2} = \frac{\tilde{v}^2(t)}{2} \frac{\pi^2}{18} \\ \langle \hat{v}_x(t) \hat{v}_y(t) \rangle_{\text{stat}} &= 0 \end{aligned} \quad (39)$$

and vanishing statistical averages

$$\langle C(t) \rangle_{\text{stat}} = 0 \quad \langle S(t) \rangle_{\text{stat}} = 0 \quad (40)$$

at *any* time t , see Eqs.(26). Therefore, by construction, this model gives a definite non-zero signal but, if the same signal were fitted with Eqs.(31) and (32), it also gives average values $(C_k)^{\text{avg}} = 0$, $(S_k)^{\text{avg}} = 0$ for the Fourier coefficients.

⁶The correct normalization Eq.(37) produces boundaries which are smaller by a factor $\frac{1}{\sqrt{2}}$ as compared to those of ref.[29] where the relation $d_x(t) = d_y(t) \sim \tilde{v}(t)$ was assumed. For this reason, in view of Eqs.(36), the resulting amplitudes of the signal are now predicted to be smaller by about a factor of 2.

Table 1: *The amplitude of the fitted second-harmonic component A_2^{EXP} for the six experimental sessions of the Michelson-Morley experiment. The table is taken from ref.[28].*

SESSION	A_2^{EXP}
July 8 (noon)	0.010 ± 0.005
July 9 (noon)	0.015 ± 0.005
July 11 (noon)	0.025 ± 0.005
July 8 (evening)	0.014 ± 0.005
July 9 (evening)	0.011 ± 0.005
July 12 (evening)	0.024 ± 0.005

4. The classical experiments in gaseous media

To fully appreciate the change of perspective implied by Eqs.(40), let us consider the traditional procedure of data taking in the classical experiments. Fringe shifts were observed at the same sidereal time on a few consecutive days so that changes in the earth orbital velocity could be ignored. Then, see Eqs.(20) and (25), the data were averaged at any given angle θ

$$\left\langle \frac{\Delta\lambda(\theta; t)}{\lambda} \right\rangle_{\text{stat}} = \frac{2L}{\lambda} [2 \sin 2\theta \langle S(t) \rangle_{\text{stat}} + 2 \cos 2\theta \langle C(t) \rangle_{\text{stat}}] \quad (41)$$

and these averages were compared with various models of cosmic motion.

But, if the ether-drift is a genuine stochastic phenomenon, as expected if the physical vacuum were similar to a turbulent fluid which becomes isotropic at small scales, these average combinations should vanish *exactly* for an infinite number of measurements. Thus, averages of vectorial quantities are non vanishing just because the statistics is finite and forming the averages Eq.(41) is not a meaningful procedure. In particular, the direction $\theta_0(t)$ of the drift in the plane of the interferometer (defined by the relation $\tan 2\theta_0(t) = S(t)/C(t)$) is a completely random quantity which has no definite limit by combining a large number of observations.

Instead, one should concentrate on the 2nd-harmonic amplitudes by comparing with

$$A_2(t) = \frac{2L}{\lambda} 2\sqrt{S^2(t) + C^2(t)} \quad (42)$$

These are positive-definite quantities and, as such, remain definitely non-zero after any averaging procedure. In addition, being rotationally invariant, their statistical properties remain the same by adopting the isotropic model Eq.(38) or the non-isotropic choice $d_x(t) \equiv \tilde{v}_x(t)$ and $d_y(t) \equiv \tilde{v}_y(t)$.

As a matter of fact, by restricting to the amplitudes, one finds [28] a good consistency of the data with the kinematical parameters obtained from the CMB observations. For instance, let us consider the experimental 2nd-harmonics extracted from the six sessions of the Michelson-Morley experiment, see Table 1.

Due to their reasonable statistical consistency, one can compute the mean and variance of the six determinations by obtaining $A_2^{\text{EXP}} \sim 0.016 \pm 0.006$. By comparing with the classical

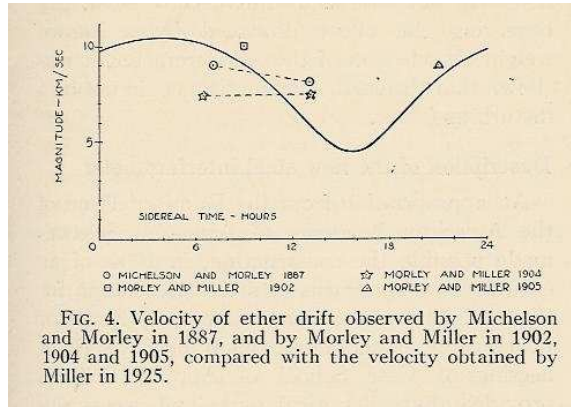


FIG. 4. Velocity of ether drift observed by Michelson and Morley in 1887, and by Morley and Miller in 1902, 1904 and 1905, compared with the velocity obtained by Miller in 1925.

Figure 2: *The magnitude of the observable velocity measured in various experiments as reported by Miller [12].*

prediction $A_2^{\text{class}} = \frac{L (30\text{km/s})^2}{\lambda c^2} \sim 0.20$, this average amplitude corresponds to an observable velocity $v_{\text{obs}} \sim (8.4 \pm 1.6)$ km/s in very good agreement with Miller's analysis, see Fig.2. Then, by using Eq.(23), for air at atmospheric pressure where $\epsilon \sim 2.8 \cdot 10^{-4}$, one obtains a true kinematical value $v \sim (355 \pm 70)$ km/s. Notice the consistency with the determination $v \sim 370$ km/s obtained from the CMB observations.

Analogously, let us consider Miller's extensive observations. After the critical re-analysis of his original measurements performed by the Shankland team [26], one has an accurate determination of the overall average for all epochs of the year (see Table III of [26]). The resulting amplitude $A_2^{\text{EXP}} = 0.044 \pm 0.022$, when compared with the equivalent classical prediction for Miller's interferometer $A_2^{\text{class}} = \frac{L (30\text{km/s})^2}{\lambda c^2} \sim 0.56$, gives $v_{\text{obs}} \sim (8.4 \pm 2.2)$ km/s and, by using Eq.(23), a true kinematical value $v \sim (355 \pm 90)$ km/s, again consistent with the CMB observations.

At the same time, the perfect identity of two determinations obtained in completely different experimental conditions (in the basement of Cleveland University or on top of Mount Wilson) indicates that the standard interpretation [26] of the residuals in terms of temperature differences in the air of the optical paths is only acceptable provided this gradient has a *non-local* origin. A natural physical interpretation will be proposed in Section 7.

Analogous considerations can be applied to the other classical experiments in gaseous helium, such as Illingworth's 1927 experiment at Caltech (sensitivity about 1/1500 of a fringe) or Joos's 1930 experiment in Jena (sensitivity about 1/3000 of a fringe). By ignoring the directional character of the data and just restricting to the amplitudes of the individual observations [28], for $\epsilon \sim 3.3 \cdot 10^{-5}$ in Eq.(23), the very low observable velocities of about 2÷3 km/s become consistent with the CMB value of 370 km/s. In particular, by using Eqs.(42) and (28) to fit the time dependence of the amplitudes extracted from Joos's observations (data collected at regular steps of one hour to cover the full sidereal day and recorded automatically by photocamera), one even gets [28] some information on the right ascension and angular declination, namely $\alpha(\text{fit} - \text{Joos}) = (168 \pm 30)$ degrees and $\gamma(\text{fit} - \text{Joos}) = (-13 \pm 14)$ degrees,

Table 2: *The average velocity observed (or the limits placed) by the classical ether-drift experiments in the alternative interpretation where the relation between the observable v_{obs} and the kinematical v is governed by Eq.(23).*

Experiment	gas in the interferometer	v_{obs} (km/s)	v (km/s)
Michelson-Morley(1887)	air	$8.4^{+1.5}_{-1.7}$	355^{+62}_{-70}
Morley-Miller(1902-1905)	air	8.5 ± 1.5	359 ± 62
Miller(1925-1926)	air	$8.4^{+1.9}_{-2.5}$	355^{+79}_{-104}
Tomaschek (1924)	air	$7.7^{+2.1}_{-2.8}$	325^{+87}_{-116}
Kennedy(1926)	helium	< 5	< 600
Illingworth(1927)	helium	$2.4^{+0.8}_{-1.2}$	295^{+98}_{-146}
Piccard-Stahel(1926-1927)	air	$6.3^{+1.5}_{-2.0}$	266^{+62}_{-83}
Michelson-Pease-Pearson(1929)	air	$4.3 \pm \dots$	$182 \pm \dots$
Joos(1930)	helium	$1.8^{+0.5}_{-0.6}$	226^{+63}_{-76}

to compare with the present values $\alpha(\text{CMB}) \sim 168$ degrees and $\gamma(\text{CMB}) \sim -7$ degrees.

The only possible discrepancy found in ref.[28] concerned the Michelson-Pease-Pearson (MPP) experiment at Mount Wilson which was giving a considerably smaller central value, namely $v \sim 180$ km/s, for the kinematical velocity, even though the associated uncertainty could not be estimated. The general situation is summarized in Table 2 where we have also included the determinations from the Tomaschek [51] and Piccard-Stahel ⁷ experiments [52]. However, we will now show that, within statistical uncertainties, also the MPP experiment can become consistent with our stochastic model.

As discussed in [28] it is extremely difficult to understand the results of the MPP experiment from the original articles [53, 54]. No numerical results are reported and the two papers are even in contradiction about the magnitude of the measured effects (“one-fifteenth” of the expected value vs. “one-fiftieth”). To try to understand, we have consulted another article which, rather surprisingly, was signed by Pease alone [55]. In this article, Pease declares that, in their experiment, to test Miller’s claims, they concentrated on a purely *differential* type of measurement. For this reason, he only reports the quantity

$$\delta(\theta) = \left\langle \frac{\Delta\lambda(\theta; t = 5 : 30)}{\lambda} \right\rangle_{\text{stat}} - \left\langle \frac{\Delta\lambda(\theta; t = 17 : 30)}{\lambda} \right\rangle_{\text{stat}}$$

This means that they were performing a large set of observations at sidereal time 5:30 and averaging the data. Then, the same procedure was carried out, in the same days, at sidereal time 17:30. Finally, the two averages were subtracted to form the quantities $\delta(\theta)$. These are typically below ± 0.004 and this is the order of magnitude which is usually compared [26]

⁷The velocities for the Piccard-Stahel experiment [52] derive from the value $D/\lambda = 6.4 \cdot 10^6$ and the average 2nd-harmonic amplitude $(2.8 \pm 1.5) \cdot 10^{-3}$. This is obtained from their individual 24 determinations namely (in units 10^{-3}), the 12 Mt.Rigi values $A_2^{\text{EXP}} = 3.4, 1.1, 4.0, 2.4, 2.4, 4.3, 2.3, 2.6, 0.6, 2.0, 1.2, 3.9$, and the 12 Brussels measurements, at night $A_2^{\text{EXP}} = 3.2, 5.2, 6.5, 2.2, 4.9, 3.8$ and in the morning $A_2^{\text{EXP}} = 1.85, 1.27, 3.40, 1.00, 3.70, 1.14$.

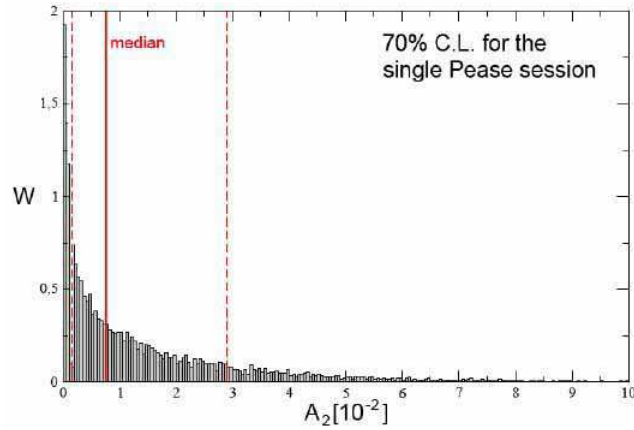


Figure 3: *The histogram W of a numerical simulation of 10,000 instantaneous amplitudes for the single session of January 13, 1928, reported by Pease [55]. The vertical normalization is to a unit area. We show the median and the 70% C.L. The limits on the random Fourier components in Eqs.(34) and (35) were fixed by the CMB kinematical parameters as explained in the text.*

with the classical expectation for the MPP apparatus, namely $A_2^{\text{class}} = \frac{L}{\lambda} \frac{(30\text{km/s})^2}{c^2} \sim 0.45$ for optical path of 85 feet or $A_2^{\text{class}} = \frac{L}{\lambda} \frac{(30\text{km/s})^2}{c^2} \sim 0.29$ for optical path of 55 feet.

As explained above, by accepting a stochastic picture of the ether-drift, the vector average of more and more observations will wash out completely the physical information contained in the original measurements. Therefore, from these δ -values, nothing can be said about the magnitude of the fringe shifts $\frac{\Delta\lambda(\theta)}{\lambda}$ obtained in the individual measurements, i.e. before any averaging procedure and before any subtraction. Pease just reports a poor-quality plot of a single observation, performed on January 13, 1928, when the length of the optical path was still 55 feet. In this plot, the fringes vary approximately in the range ± 0.006 whose absolute value may be taken to estimate the amplitude of that observation.

We have thus performed a numerical simulation in our stochastic model by generating 10,000 values of the amplitude, at the same sidereal time 5:30 of the observation reported by Pease, and using the CMB kinematical parameters to bound the random Fourier components of the velocity field Eqs.(34) and (35). The resulting histogram, reported in Fig.3, shows that the value $A_2 \sim 0.006$ lies well within the 70% Confidence Limit. Notice the large probability content at very small amplitudes ⁸ and the long tail extending up to $A_2 = 0.030$ or even larger values.

The wide interval of amplitudes corresponding to the 70% C. L. (which could be expressed as $0.014_{-0.012}^{+0.015}$) indicates that, in our stochastic model, one could accommodate individual MPP

⁸Strictly speaking, for a more precise comparison with the data, one should fold the histogram with a smearing function which takes into account the finite resolution Δ of the apparatus. The resulting curve will bend for $A_2 \rightarrow 0$ and saturate to a limit which depends on Δ . Nevertheless, this refinement should not modify substantially the probability content around the median which is very close to $A_2 = 0.007$.

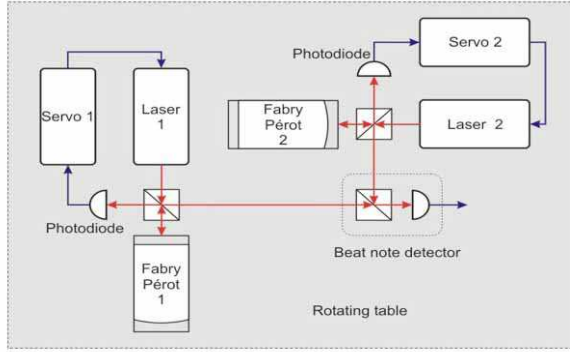


Figure 4: *The scheme of a modern ether-drift experiment. The light frequencies are first stabilized by coupling the lasers to Fabry-Pérot optical resonators. The frequencies ν_1 and ν_2 of the signals from the resonators are then compared in the beat note detector which provides the frequency shift $\Delta\nu = \nu_1 - \nu_2$. In present experiments a very high vacuum is maintained within the resonators.*

observations with an amplitude as 0.002 or as 0.030 which is fifteen times larger. This is another crucial difference with a deterministic model of the ether-drift. In this traditional view, in fact, the amplitude can vary at most by a factor $r = (v_{\max}/v_{\min})^2$ where v_{\max} and v_{\min} are respectively the maximum and minimum daily projection of the earth velocity in the interferometer plane. Therefore, since r varies typically by a factor of two, the observation of such large fluctuations in the data would induce to conclude, in a deterministic model, that there must be some systematic effect which modifies the measurements in an uncontrolled way.

This confirms the overall consistency of our picture with the classical experiments and should induce to perform the new dedicated experiments where the optical resonators which are coupled to the lasers (see Fig.4) are filled by gaseous media. In this case, from Eq.(8), one should compare the data with the prediction

$$\frac{\Delta\nu(\theta)}{\nu_0} = \frac{\Delta\bar{c}_\theta}{c} \sim \epsilon \frac{v^2}{c^2} \cos 2(\theta - \theta_0) \quad (43)$$

These experiments will likely require a good deal of ingenuity and technical skill. For instance, an important element to increase the overall stability and minimize systematic effects may consist in obtaining the two optical resonators from the same block of material as with the crossed optical cavity of ref.[56]. Still, measuring precisely the frequency shift in the gas mode will be a delicate issue. To fix the ideas, let us consider gaseous helium at atmospheric pressure, a velocity $v = 300$ km/s and a typical laser frequency of about $3 \cdot 10^{14}$ Hz. In these conditions, the expected shift is $\Delta\nu \sim 10$ kHz. This is much smaller than many effects which must preliminarily be subtracted. For instance, by changing from vacuum to the gas case under pressure, and for a typical cavity length of 10 cm, the effect of cavity deformations is about 10 MHz [57]. Theoretically, this should not depend on the gas used but only on the solid parts of the apparatus. Yet, experimental measurements at

atmospheric pressure show that there is a difference between Nitrogen and Helium of about 0.6 MHz [57]. Therefore, one should lower the pressure to reduce this spurious effect. Of course, this is what might show up in a single cavity while we are interested in the frequency shift between two cavities where the effect will be reduced. Nevertheless, the pressure will have to be lowered and, then, also the signal will be reduced correspondingly. Therefore, several technical problems must be solved before concluding that, in the gas case, there is a definite improvement with respect to the classical experiments (in particular with respect to Joos).

However, at present, a first rough check of Eq.(43) can be obtained from the time variation of the signal observed in the only modern experiment performed in similar conditions, namely the 1963 MIT experiment by Jaseja et. al [58] with He-Ne lasers. At that time, the laser stabilization mechanism had not yet been invented and one was just comparing directly the frequencies of the two lasers. As a matter of fact, for a laser frequency $\nu_0 \sim 2.6 \cdot 10^{14}$ Hz, the residual observed variations of a few kHz are consistent with the refractive index $\mathcal{N}_{\text{He-Ne}} \sim 1.00004$ and the typical change of the earth cosmic velocity at the latitude of Boston. For more details, see the discussion given in [59].

Meanwhile, waiting for the new dedicated experiments, one can try to have a different check with vacuum experiments. The point is that, as illustrated in the next section, for the physical vacuum the equality $\mathcal{N}_v = 1$ might not be exact.

5. An effective refractivity for the physical vacuum

The idea of an effective refractivity for the physical vacuum becomes natural by adopting a different view of the curvature effects observed in a gravitational field.

The usual perspective, derived from General Relativity, is that these effects require the introduction of a non-trivial metric field $g_{\mu\nu}(x)$ viewed as a fundamental modification of Minkowski space-time. By *fundamental*, we mean that deviations from flat space might also occur at extremely small scales, in principle comparable to the Planck length. Though, it is an experimental fact that many physical systems for which, at a fundamental level, space-time is exactly flat are nevertheless described by an effective curved metric in their hydrodynamic limit, i.e. at length scales that are much larger than the size of their elementary constituents.

For this reason several authors, see e.g. [60, 61, 62, 63], have started to explore those gravity-analogs (moving fluids, condensed matter systems with a refractive index, Bose-Einstein condensates,...) which are known in flat space. The ultimate goal is that, as with the deflection of light in Euclidean space when propagating in a medium of variable density, one might succeed to explain the curvature effects in a gravitational field in terms of the hydrodynamic excitations of an underlying form of (quantum) ether.

We believe that there is a value in this attempt. In fact, beyond the simple level of an analogy, there might be a deeper significance if the properties of the underlying medium could be matched with those of the physical vacuum of electroweak and strong interactions. In this case, the so called vacuum condensates, which play a crucial role for fundamental phenomena such as mass generation and quark confinement, could also represent a bridge

between gravity and particle physics [64].

To be more definite, suppose that gravity originates from some long-range fields $s_k(x)$. By this we mean that their typical wavelengths are larger than some minimal scale (consistently with the experimental verifications [65] of the 1/r law) and that the deviation of the effective $g_{\mu\nu}(x)$ from the Minkowski tensor $\eta_{\mu\nu}$ can be expressed as

$$g_{\mu\nu}(x) - \eta_{\mu\nu} = \delta g_{\mu\nu}[s_k(x)] \quad (44)$$

with $\delta g_{\mu\nu}[s_k = 0] = 0$. In this type of approach, as in the original Yilmaz derivation [66], Einstein's equations for the metric should be considered as algebraic identities which follow directly from the equations of motion for the s_k 's in flat space, after introducing a suitable stress tensor for these inducing-gravity fields⁹. In this way, one could (partially) fill the conceptual gap with classical General Relativity. As an immediate consequence, if the s_k 's represent *excitations* of the physical vacuum, which therefore vanish identically in the equilibrium state, one could easily understand [62] why the huge condensation energy of the unperturbed vacuum plays no role, thus obtaining an intuitive solution of the cosmological-constant problem found in connection with the energy of the quantum vacuum¹⁰.

This is not the place to discuss the various pros and cons of this type of approach. Instead, in our context of the ether-drift experiments, we will explore some possible phenomenological consequence. To this end, let us assume a zeroth-order model of gravity with a scalar field $s_0(x)$ which, at least on some coarse-grained scale, behaves as the Newtonian potential. Then, how could its effects be effectively re-absorbed into a curved metric structure? At a pure kinematical level and regardless of the detailed dynamical mechanisms, the standard basic ingredients would be: 1) space-time dependent modifications of the physical clocks and rods and 2) space-time dependent modifications of the velocity of light. This point of view can be well represented by the following two citations:

Citation 1:

“It is possible, on the one hand, to postulate that the velocity of light is a universal constant, to define *natural* clocks and measuring rods as the standards by which space and time are to be judged and then to discover from measurement that space-time is *really* non-Euclidean. Alternatively, one can *define* space as Euclidean and time as the same everywhere, and discover (from exactly the same measurements) how the velocity of light and natural clocks, rods and particle inertias *really* behave in the neighborhood of large masses” [69].

Citation 2:

“Is space-time really curved? Isn't it conceivable that space-time is actually flat, but clocks and rulers with which we measure it, and which we regard as perfect, are actually rubbery? Might not even the most perfect of clocks slow down or speed up and the most

⁹In the simplest, original Yilmaz approach [66] there is only one inducing-gravity field $s_0(x)$ which plays the role of the Newtonian potential. Introducing its stress tensor $t_\nu^\mu(s_0) = -\partial^\mu s_0 \partial_\nu s_0 + 1/2 \delta_\nu^\mu \partial^\alpha s_0 \partial_\alpha s_0$, to match the Einstein tensor, produces differences from the Schwarzschild metric which are beyond the present experimental accuracy, see [67].

¹⁰In this sense, with this approach one is taking seriously Feynman's indication that “the first thing we should understand is how to formulate gravity so that it doesn't interact with the vacuum energy” [68].

perfect of rulers shrink or expand, as we move them from point to point and change their orientations? Would not such distortions of our clocks and rulers make a truly flat space-time appear to be curved? Yes.”[70]

Therefore, within this interpretation of the space-time curvature, one might wonder about the fundamental assumption of General Relativity that, even in the presence of gravity, the velocity of light in vacuum c_γ is a universal constant, namely it remains the same, basic parameter c entering Lorentz transformations. Notice that, here, we are not considering the so called coordinate-dependent speed of light. Rather, our interest is focused on the value of the true, physical c_γ as, for instance, obtained from experimental measurements in vacuum optical cavities placed on the earth surface.

To understand the various aspects, a good reference is Cook’s article “Physical time and physical space in general relativity” [71]. This article makes extremely clear which definitions of time and length, respectively $d\tau$ and dl , are needed if all observers have to measure the same, universal speed of light (“Einstein postulate”). For a static metric, these definitions are $d\tau^2 = g_{00}dt^2$ and $dl^2 = g_{ij}dx^i dx^j$. Thus, in General Relativity, the condition $ds^2 = 0$, which governs the propagation of light, can be expressed formally as

$$ds^2 = c^2 d\tau^2 - dl^2 = 0 \quad (45)$$

and, by construction, yields always the same universal speed $c = dl/d\tau$.

For the same reason, however, if the physical units of time and space were instead defined to be $d\hat{\tau}$ and $d\hat{l}$ with, say, $d\tau = q d\hat{\tau}$ and $dl = p d\hat{l}$, the same condition

$$ds^2 = c^2 q^2 d\hat{\tau}^2 - p^2 d\hat{l}^2 = 0 \quad (46)$$

would now be interpreted in terms of the different speed

$$c_\gamma = \frac{d\hat{l}}{d\hat{\tau}} = c \frac{q}{p} \equiv \frac{c}{\mathcal{N}_v} \quad (47)$$

The possibility of different standards for space-time measurements is thus a simple motivation for an effective vacuum refractive index $\mathcal{N}_v \neq 1$. As we are going to illustrate, this scenario can be tested and shown to be consistent with present ether-drift experiments.

For sake of clarity, we shall start our analysis from the unambiguous point of view of special relativity: the right space-time units are those for which the speed of light in the vacuum c_γ , when measured in an inertial frame, coincides with the basic parameter c entering Lorentz transformations. However, inertial frames are just an idealization. Therefore the appropriate realization is to assume *local* standards of distance and time such that the identification $c_\gamma = c$ holds as an asymptotic relation in the physical conditions which are as close as possible to an inertial frame, i.e. *in a freely falling frame* (at least by restricting light propagation to a space-time region small enough that tidal effects of the external gravitational potential $U_{\text{ext}}(x)$ can be ignored). This is essential to obtain an operational definition of the otherwise *unknown* parameter c .

With this premise, as already discussed in ref.[42], light propagation for an observer S' sitting on the earth surface can be described with increasing degrees of accuracy starting from step i), through ii) and finally arriving to iii):

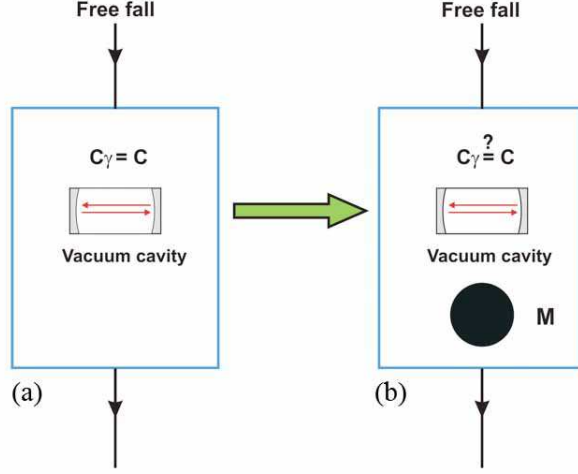


Figure 5: A pictorial representation of the effect of a heavy mass M carried on board of a freely-falling system, case (b). With respect to the ideal case (a), the mass M modifies the local space-time units and could introduce a vacuum refractivity so that now $c_\gamma \neq c$.

i) S' is considered a freely falling frame. This amounts to assume $c_\gamma = c$ so that, given two events which, in terms of the local space-time units of S' , differ by (dx, dy, dz, dt) , light propagation is described by the condition (ff='free-fall')

$$(ds^2)_{\text{ff}} = c^2 dt^2 - (dx^2 + dy^2 + dz^2) = 0 \quad (48)$$

ii) To a closer look, however, an observer S' placed on the earth surface can only be considered a freely-falling frame up to the presence of the earth gravitational field. Its inclusion can be estimated by considering S' as a freely-falling frame, in the same external gravitational field described by $U_{\text{ext}}(x)$, that however is also carrying on board a heavy object of mass M (the earth mass itself) which affects the local space-time structure, see Fig.5. To derive the required correction, let us denote by δU the extra Newtonian potential produced by the heavy mass M at the experimental set up where one wants to describe light propagation. Let us also denote by (dx, dy, dz, dt) the coordinate differences of the two chosen events (which for $M = 0$ coincide with the local space-time units of the freely-falling observer). According to General Relativity, and to first order in δU , light propagation for the S' observer is now described by

$$ds^2 = c^2 dt^2 \left(1 - 2 \frac{|\delta U|}{c^2}\right) - (dx^2 + dy^2 + dz^2) \left(1 + 2 \frac{|\delta U|}{c^2}\right) \equiv c^2 d\tau^2 - dl^2 = 0 \quad (49)$$

where $d\tau^2 = \left(1 - 2 \frac{|\delta U|}{c^2}\right) dt^2$ and $dl^2 = \left(1 + 2 \frac{|\delta U|}{c^2}\right) (dx^2 + dy^2 + dz^2)$ are the physical units of General Relativity in terms of which one obtains the same universal value $dl/d\tau = c_\gamma = c$.

Though, to check experimentally the assumed identity $c_\gamma = c$ one should compare with a theoretical prediction for $(c - c_\gamma)$ and thus *necessarily* modify some formal ingredient of

General Relativity. As a definite example, let us maintain the same definition of the unit of length but change the unit of time. The reason derives from the observation that physical units of time scale as inverse frequencies and that the measured frequencies $\hat{\omega}$ for $\delta U \neq 0$, when compared to the corresponding value ω for $\delta U = 0$, are red-shifted according to

$$\hat{\omega} = \left(1 - \frac{|\delta U|}{c^2}\right) \omega \quad (50)$$

Therefore, rather than the *natural* unit of time $d\tau = \left(1 - \frac{|\delta U|}{c^2}\right)dt$ of General Relativity, one could consider the alternative, but natural (see our Citation 1), unit of time

$$d\hat{t} = \left(1 + \frac{|\delta U|}{c^2}\right) dt \quad (51)$$

Then, to reproduce Eq.(49), we can introduce a vacuum refractive index

$$\mathcal{N}_v \sim 1 + 2\frac{|\delta U|}{c^2} \quad (52)$$

so that the *same* Eq.(49) takes the form ($dl^2 \equiv (d\hat{x}^2 + d\hat{y}^2 + d\hat{z}^2)$)

$$ds^2 = \frac{c^2 d\hat{t}^2}{\mathcal{N}_v^2} - (d\hat{x}^2 + d\hat{y}^2 + d\hat{z}^2) = 0 \quad (53)$$

This gives $dl/d\hat{t} = c_\gamma = \frac{c}{\mathcal{N}_v}$ and, for an observer placed on the earth surface, a refractivity

$$\epsilon_v = \mathcal{N}_v - 1 \sim \frac{2G_N M}{c^2 R} \sim 1.4 \cdot 10^{-9} \quad (54)$$

M and R being respectively the earth mass and radius.

Notice that, with this natural definition $d\hat{t}$, the vacuum refractive index associated with a Newtonian potential is the same usually reported in the literature, at least since Eddington's 1920 book [72], to explain in flat space the observed deflection of light in a gravitational field. The same expression is also suggested by the formal analogy of Maxwell equations in General Relativity with the electrodynamics of a macroscopic medium with dielectric function and magnetic permeability [73] $\epsilon_{ik} = \mu_{ik} = \sqrt{-g} \frac{(-g^{ik})}{g_{00}}$. Indeed, in our case, from the relations $g^{il} g_{lk} = \delta_k^i$, $(-g^{ik}) \sim \delta_k^i g_{00}$, $\epsilon_{ik} = \mu_{ik} = \delta_k^i \mathcal{N}_v$, we obtain

$$\mathcal{N}_v \sim \sqrt{-g} \sim \sqrt{\left(1 - 2\frac{|\delta U|}{c^2}\right)\left(1 + 2\frac{|\delta U|}{c^2}\right)^3} \sim 1 + 2\frac{|\delta U|}{c^2} \quad (55)$$

A difference is found with Landau's and Lifshitz' textbook [74] where the vacuum refractive index entering the constitutive relations is instead defined as $\mathcal{N}_v \sim \frac{1}{\sqrt{g_{00}}} \sim 1 + \frac{|\delta U|}{c^2}$. This alternative definition ¹¹ corresponds to a different choice of the physical units and can also be taken into account as a theoretical uncertainty. We emphasize that this difference by a factor of 2 is not really essential. The main point is that c_γ , as measured in a vacuum cavity on the earth surface (panel **(b)** in our Fig.5), could differ at a fractional level 10^{-9} from the

¹¹A very complete set of references to these two possible alternatives for the vacuum refractive index in gravitational field is given by Broekaert [75], see his footnote ³.

ideal value c , as operationally defined with the same apparatus in a true freely-falling frame (panel **(a)** in our Fig.5). In conclusion, this $c_\gamma - c$ difference can be conveniently expressed through a vacuum refractivity of the form

$$\epsilon_v = \mathcal{N}_v - 1 \sim \frac{z}{2} 1.4 \cdot 10^{-9} \quad (56)$$

where the factor $z/2$ (with $z=1$ or 2) takes into account the mentioned theoretical uncertainty.

iii) Could one check experimentally if $\mathcal{N}_v \neq 1$? Today, the speed of light in vacuum is assumed to be a fixed number with no error, namely 299 792 458 m/s. Thus if, for instance, this estimate were taken to represent the value measured on the earth surface, in our picture and in an ideal freely-falling frame there should be a slight increase, namely $+\frac{z}{2}(0.42)$ m/s with $z = 1$ or 2 . It seems hopeless to measure unambiguously such a difference because the uncertainty of the last precision measurements performed before the “exactness” assumption had precisely this order of magnitude, namely $\pm 4 \cdot 10^{-9}$ at the 3-sigma level or, equivalently, ± 1.2 m/s [76].

Therefore, as pointed out in ref.[42], an experimental test cannot be obtained from the value of the average isotropic speed but, rather, from a possible *anisotropy* associated with a theoretical difference between c_γ and c . In fact, with a preferred frame, and if $\mathcal{N}_v \neq 1$, an isotropic light propagation as in Eq.(53) can only be valid for a special state of motion of the earth laboratory. This provides the definition of Σ while for a non-zero relative velocity \mathbf{V} there are off diagonal elements $g_{0i} \neq 0$ in the effective metric [73]. The resulting two-way velocity would then be given by Eq.(16) with ϵ as in Eq.(56). On the basis of Eq.(19), and for the typical $v \sim 370$ km/s, we then expect a light anisotropy $\frac{|\Delta \bar{c}_\theta|}{c} \sim (\mathcal{N}_v - 1)(v/c)^2 \sim 10^{-15}$. As a matter of fact, this prediction is consistent with the presently most precise room-temperature vacuum experiment of ref. [23] and with the cryogenic vacuum experiment of ref.[22]. In particular, in the latter case this measured 10^{-15} level was about 100 times larger than the designed $O(10^{-17})$ short-term stability.

6. Simulations of experiments with vacuum optical resonators

Most recent ether-drift experiments measure the frequency shift $\Delta\nu$ of two *rotating* optical resonators. To this end, let us re-write Eq.(24) as

$$\frac{\Delta\nu(t)}{\nu_0} = \frac{\Delta \bar{c}_\theta(t)}{c} \sim \epsilon \frac{v^2(t)}{c^2} \cos 2(\omega_{\text{rot}} t - \theta_0(t)) \quad (57)$$

where ω_{rot} is the rotation frequency of the apparatus. Therefore one finds

$$\frac{\Delta\nu(t)}{\nu_0} \sim 2S(t) \sin 2\omega_{\text{rot}} t + 2C(t) \cos 2\omega_{\text{rot}} t \quad (58)$$

with $C(t)$ and $S(t)$ given in Eqs.(26).

To estimate the signal expected with vacuum optical resonators, we have performed several numerical simulations in the isotropic stochastic model of Sect.3 with ϵ_v fixed as in

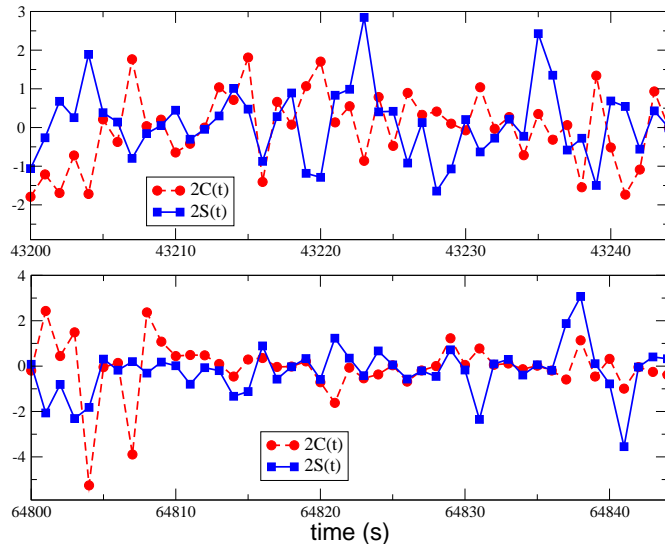


Figure 6: *Two typical sets of 45 seconds for the instantaneous $2C(t)$ and $2S(t)$ in units 10^{-15} . The two sets belong to the same random sequence and refer to two sidereal times that differ by 6 hours. The boundaries of the stochastic velocity components in Eqs.(34) and (35) are controlled by $(V, \alpha, \gamma)_{\text{CMB}}$ through Eqs.(28) and (38). For a laser frequency of $2.8 \cdot 10^{14}$ Hz [23], the interval $\pm 3 \cdot 10^{-15}$ corresponds to a typical frequency shift $\Delta\nu$ in the range ± 1 Hz.*

Eq.(56) for $z = 2$. However, the theoretical uncertainty associated with the two possible choices $z = 1$ or 2 is also taken into account in the final formulas.

We first report in Fig.6 two typical sets for $2C(t)$ and $2S(t)$ during one rotation period $T_{\text{rot}} = 45$ seconds of the apparatus of ref.[20]. The two sets belong to the same random sequence and refer to two sidereal times that differ by 6 hours. The set $(V, \alpha, \gamma)_{\text{CMB}}$ was adopted to control the boundaries of the stochastic velocity components through Eqs.(27), (28) and (38). The value $\phi = 52$ degrees was also fixed to reproduce the average latitude of the laboratories in Berlin and Düsseldorf. For a laser frequency of $2.8 \cdot 10^{14}$ Hz [23], the interval $\pm 3 \cdot 10^{-15}$ of these dimensionless amplitudes corresponds to a random instantaneous frequency shift $\Delta\nu$ in the typical range ± 1 Hz. This is well consistent with the signal observed in ref.[23], see their Fig.4.

To compare with data extending over longer time intervals one has first to take into account the large, long-term drift which affects the experimental frequency shift. For instance, for the presently most precise experiment of ref.[23], for time variations of several hours this drift is about ± 500 Hz, see their Fig.3 (top part). This is about 1000 times larger than the typical signal expected in our model, thus suggesting that we might be forced to abandon altogether the possibility of a precision test of our picture.

However, a way out derives from the observation that, although the frequency shift changes by such a large amount, still one can correct the data in order to achieve a much better stability. Indeed, by suitable modeling and subtraction of the drift, the typical variation of the shift over 1 second becomes about ± 0.24 Hz (see their Fig.3, bottom part) and

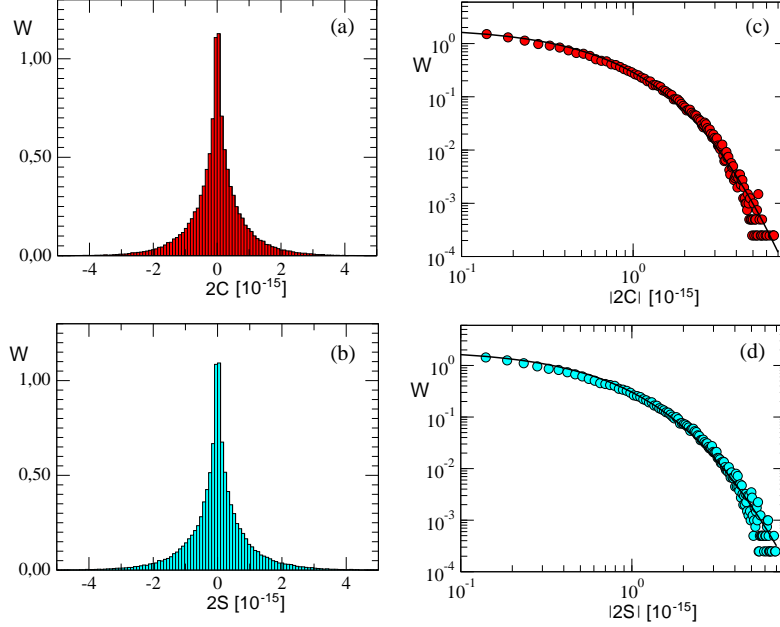


Figure 7: We show, see (a) and (b), the histograms W obtained from a single simulation of instantaneous measurements of $2C = 2C(t)$ and $2S = 2S(t)$ generated at regular steps of 1 second over an entire sidereal day. The vertical normalization is to a unit area. The mean values are $2C_0 = \langle 2C \rangle_{\text{day}} = -1.6 \cdot 10^{-18}$, $2S_0 = \langle 2S \rangle_{\text{day}} = 4.3 \cdot 10^{-18}$ and the standard deviations $\sigma(2C) = 8.7 \cdot 10^{-16}$, $\sigma(2S) = 9.6 \cdot 10^{-16}$. We also show, see (c) and (d), the corresponding plots in a log-log scale and the fits with Eq.(63). The boundaries of the stochastic velocity components in Eqs.(34) and (35) are controlled by $(V, \alpha, \gamma)_{\text{CMB}}$ through Eqs.(28) and (38).

thus at the level $\pm 8 \cdot 10^{-16}$. This means that, after correcting the data, the *local* properties of the signal, i.e. its characteristic variations over a time scale of 1 second, depend on the possible times $t_i, t_j, t_k \dots$ of the observations to a negligible extent as compared to the original differences among the corresponding $\Delta\nu(t_i), \Delta\nu(t_j), \Delta\nu(t_k) \dots$. Then, even if these were differing by a large amount, we can now get a test at the 10^{-15} level.

To compare with such a high short-term stability, we have thus simulated sequences of instantaneous measurements performed at regular steps of 1 second over an entire sidereal day. With such a type of simulation, we can also get an idea of the C_k and S_k , entering Eqs.(31) and (32), for a large but finite statistics (where one cannot get exactly zero as expected from Eqs.(39) and (40)). For a particular random sequence, the resulting histograms of $2C$ and $2S$ are reported in panels (a) and (b) of Fig.7.

In view of Eqs.(39) and (40) the non-zero averages $\langle 2C \rangle_{\text{day}} = 2C_0 = \mathcal{O}(10^{-18})$, $\langle 2S \rangle_{\text{day}} = 2S_0 = \mathcal{O}(10^{-18})$ should only be considered as statistical fluctuations around zero. The same holds true for the other C_k and S_k Fourier coefficients in Eqs.(31) and (32). By fitting the generated distributions to Eqs.(31) and (32) one gets values which are also $\mathcal{O}(10^{-18})$ or smaller and which fluctuate randomly around zero as expected. This simulated pattern is

in complete agreement with the typical magnitude $\mathcal{O}(10^{-18})$ obtained in ref.[23] from the experimental data.

On the other hand, in such simulations of one-day measurements at steps of one second, the standard deviations around the 10^{-18} averages, say $\sigma_{\text{th}}(2C)$ and $\sigma_{\text{th}}(2S)$, are very stable ($z = 1$ or 2)

$$[\sigma_{\text{th}}(2C)]_{1\text{-second}} \sim \frac{z}{2}(8.7 \pm 0.8) \cdot 10^{-16} \quad [\sigma_{\text{th}}(2S)]_{1\text{-second}} \sim \frac{z}{2}(9.6 \pm 0.9) \cdot 10^{-16} \quad (59)$$

Here the \pm uncertainties reflect the observed variations due to the truncation of the Fourier modes in Eqs.(34), (35) and to the dependence on the random sequence.

From Eq.(58), by combining quadratically these two sigma's, we estimate

$$\left[\sigma_{\text{th}}\left(\frac{\Delta\nu}{\nu_0}\right) \right]_{1\text{-second}} \sim \frac{z}{2}(9 \pm 1) \cdot 10^{-16} \quad (60)$$

so that, for a laser frequency $\nu_0 = 2.8 \cdot 10^{14}$ Hz [23], we expect a typical spread

$$[\sigma_{\text{th}}(\Delta\nu)]_{1\text{-second}} \sim \frac{z}{2}(0.26 \pm 0.02) \text{ Hz} \quad (61)$$

of the frequency shift measured every 1 second over a one-day period. For $z = 2$, this estimate is in very good agreement with the mentioned experimental value

$$[\sigma_{\text{exp}}(\Delta\nu)]_{1\text{-second}} \sim 0.24 \text{ Hz} \quad (62)$$

which is reported in ref.[23] for an integration time of 1 second. Therefore, to the present best level of accuracy, this agreement strongly favours the value $z = 2$, which is the only free parameter of our scheme.

Our estimates are also well consistent with the analogous (but slightly less stringent) limit $\sigma_{\text{exp}}(\frac{\Delta\nu}{\nu_0}) \sim 1.5 \cdot 10^{-15}$, at $1 \div 2$ seconds, placed by the cryogenic experiment of ref.[22]. Notice that this measured 10^{-15} level was about 100 times larger than the expected $\mathcal{O}(10^{-17})$ short-term stability. However, by the authors of ref.[22], it was interpreted as a spurious effect due to a lack of rigidity of their cryostat. Probably, they have not considered the possibility of a genuine random signal and of intrinsic limitations placed by the vacuum structure.

We emphasize that the generated distributions are very different from a Gaussian shape, an aspect which is characteristic of probability distributions for instantaneous data in turbulent flows (see e.g. [77, 78]). To better appreciate the deviation from Gaussian behavior, in panels (c) and (d) we plot the same data in a log–log scale. The resulting distributions are well fitted by the so-called q –exponential function [79]

$$f_q(x) = a(1 - (1 - q)xb)^{1/(1-q)} \quad (63)$$

with “entropic” index $q \sim 1.1$. This explains why, by performing extensive simulations, there might be occasionally large spikes of the instantaneous amplitude, up to $7 \cdot 10^{-15}$ or larger, when many Fourier modes sum up coherently (see the tails in panels (c) and (d) of Fig.7). The effect of these spikes, which lie at about 7 sigma's in terms of the standard deviations Eq.(59), gets smoothed when averaging but their non-negligible presence (about 10^{-4} probability) is

characteristic of the stochastic model. Otherwise, for a Gaussian distribution, 7 sigma's would correspond to a 10^{-11} probability.

As already observed for the classical experiments, another reliable indicator is the statistical average of the quadratic amplitude of the signal

$$A(t) \equiv 2\sqrt{S^2(t) + C^2(t)}$$

which is a positive-definite quantity and, as such, remains definitely non-zero after any averaging procedure. In this case, by using Eqs. (56) and (39), one finds ($z = 1$ or 2)

$$\langle A^{\text{th}}(t) \rangle_{\text{stat}} = \epsilon_v \frac{\tilde{v}^2(t)}{c^2} \frac{1}{3} \sum_{n=1}^{\infty} \frac{1}{n^2} = \frac{z}{2} (7.7 \cdot 10^{-16}) \frac{\tilde{v}^2(t)}{(300 \text{ km/s})^2} \quad (64)$$

By maintaining the CMB parameters $(V, \alpha, \gamma)_{\text{CMB}}$ and fixing $\phi = 52$ degrees, one gets a daily average $\sqrt{\langle \tilde{v}^2 \rangle}_{\text{day}} \sim 332 \text{ km/s}$ from the relation [42]

$$\langle \tilde{v}^2 \rangle_{\text{day}} = V^2 \left(1 - \sin^2 \gamma \sin^2 \phi - \frac{1}{2} \cos^2 \gamma \cos^2 \phi \right) \quad (65)$$

Thus, we predict a daily average amplitude ($z = 1$ or 2)

$$\langle A^{\text{th}} \rangle_{\text{day}} \sim \frac{z}{2} 9 \cdot 10^{-16} \quad (66)$$

that, for a laser frequency $2.8 \cdot 10^{14} \text{ Hz}$, corresponds again to a typical instantaneous frequency shift $|\Delta\nu|_{\text{th}} \sim \frac{z}{2} 0.26 \text{ Hz}$.

Other tests of the model will be possible if, besides the results of fits to the standard parameterizations Eqs. (31) and (32), also the basic instantaneous amplitudes $A(t)$, $S(t)$ and $C(t)$ will become available. By comparing with these genuine data, we could also get other insights and improve on our simplest model of stochastic turbulence.

To conclude, we observe that a crucial test of our model consists in detecting tiny daily variations of the amplitude. This is a very difficult task due to the necessity of subtracting the mentioned systematic long-term drift which is much larger than the variation of a small fraction of Hz expected in our picture. Nevertheless, assuming that this subtraction could be done unambiguously to appreciate differences at the relative level 10^{-16} , for the CMB parameters at the latitude of Berlin-Düsseldorf, where the scalar velocity $\tilde{v}(t)$ in Eq.(28) changes in the range $260 \div 370 \text{ km/s}$, from Eq.(64) we expect the typical range ($z = 1$ or 2)

$$\langle A^{\text{th}}(t) \rangle_{\text{stat}} = \frac{z}{2} (9 \pm 3) \cdot 10^{-16} \quad (67)$$

More generally, if a daily variation of the amplitude will be detected, one could try to fit from the data the kinematical parameters (V, α, γ) entering Eq.(28).

7. Gaseous media vs. vacuum and solid dielectrics

7.1 Light anisotropy in gases as a non local thermal effect

Now, returning to the gas case, it is natural to ask: independently of all symmetry arguments, why there should be a non-zero light anisotropy in the earth laboratory where (the container

of) the gas is at rest? Moreover, only the region of refractive index infinitesimally close to the ideal vacuum $\mathcal{N} = 1$ has been analyzed. What about experiments performed in the other region where \mathcal{N} differs substantially from unity, as in solid dielectrics?

By concentrating on the first question, our explanation will consist in a non-local temperature gradient of a fraction of millikelvin associated with the earth motion. This idea comes out naturally by recalling that from the relation

$$\left[\frac{\Delta \bar{c}_\theta}{c} \right]_{\text{gas}} \sim (\mathcal{N}_{\text{gas}} - 1) \frac{v^2}{c^2} \cos 2\theta \quad (68)$$

and correcting with the different refractive indexes, respectively $(\mathcal{N}_{\text{air}} - 1) \sim 2.8 \cdot 10^{-4}$ and $(\mathcal{N}_{\text{helium}} - 1) \sim 3.3 \cdot 10^{-5}$, the same typical *kinematical* velocity $v \sim 300$ km/s can account for the observed light anisotropy, namely $\frac{|\Delta \bar{c}_\theta|}{c} = \mathcal{O}(10^{-10})$ for air and to $\frac{|\Delta \bar{c}_\theta|}{c} = \mathcal{O}(10^{-11})$ for helium. Therefore since, for all practical purposes, a possible non-zero vacuum anisotropy $(\mathcal{N}_v - 1)(v/c)^2 \lesssim 10^{-15}$ is irrelevant, the answer to our first question requires to find the mechanism which *enhances* substantially the anisotropy in the gas case.

To this end, it is natural to exploit the traditional *thermal* interpretation of the residuals of the classical experiments. This old argument, which gave the main motivation for Kennedy's replacement of air with gaseous helium in his optical paths, will now be illustrated by the explicit calculation of the temperature dependence of the gas refractive index \mathcal{N} .

The starting point is the Lorentz-Lorentz equation (see e.g. [57])

$$\frac{\mathcal{N}^2 - 1}{\mathcal{N}^2 + 3} = A_R \rho + B_R \rho^2 \dots \quad (69)$$

where ρ is the molar density and $A_R = (4/3)\pi N_A \alpha$ is expressed in terms of the Avogadro number N_A and of the molecular polarizability α . The coefficient B_R takes into account two-body interactions and in our case, of air and helium at atmospheric pressure, this higher order term is completely negligible. Since \mathcal{N} is very close to unity, we obtain the simplified formula for the gas refractivity

$$\epsilon = \mathcal{N} - 1 \sim \frac{3}{2} A_R \rho \quad (70)$$

In the ideal-gas approximation, the molar density at Standard Temperature and Pressure (atmospheric pressure and zero centigrade or 273.15 K) has the well known value

$$\rho(STP) = \frac{P}{RT} = \frac{101325}{(8.314)(273.15)} \text{ mol} \cdot \text{m}^{-3} \sim 4.46 \cdot 10^{-5} \text{ mol} \cdot \text{cm}^{-3} \quad (71)$$

Thus, for instance, for helium at STP and a wavelength $\lambda = 633$ nm, where $A_R \sim 0.52 \text{ mol}^{-1} \cdot \text{cm}^3$ [57], one finds $\epsilon \sim 3.5 \cdot 10^{-5}$.

The interesting aspect is that, in the ideal-gas approximation, the variation of the refractivity with the temperature has the very simple expression

$$-\frac{\partial \epsilon}{\partial T} \sim \frac{3}{2} A_R \frac{P}{RT^2} \sim \frac{\epsilon}{T} \quad (72)$$

Table 3: *The average 2nd-harmonic amplitude observed in various classical ether-drift experiments and the resulting temperature difference obtained from Eqs.(75) and (76).*

Experiment	gas	A_2^{EXP}	$\frac{2D}{\lambda}$	ΔT^{EXP} (mK)
Michelson-Morley(1887)	air	$(1.6 \pm 0.6) \cdot 10^{-2}$	$4 \cdot 10^7$	0.40 ± 0.15
Miller(1925-1926)	air	$(4.4 \pm 2.2) \cdot 10^{-2}$	$1.12 \cdot 10^8$	0.39 ± 0.20
Illingworth(1927)	helium	$(2.2 \pm 1.7) \cdot 10^{-4}$	$7 \cdot 10^6$	0.29 ± 0.22
Tomaschek (1924)	air	$(1.0 \pm 0.6) \cdot 10^{-2}$	$3 \cdot 10^7$	0.33 ± 0.20
Piccard-Stahel(1928)	air	$(2.8 \pm 1.5) \cdot 10^{-3}$	$1.28 \cdot 10^7$	0.22 ± 0.12
Joos(1930)	helium	$(1.4 \pm 0.8) \cdot 10^{-3}$	$7.5 \cdot 10^7$	0.17 ± 0.10

Therefore, by recalling the definition Eq.(17), a small temperature difference $\Delta T(\theta)$ induces a light anisotropy of typical magnitude

$$\frac{|\Delta \bar{c}_\theta|}{c} \sim |\bar{\mathcal{N}}(\theta) - \bar{\mathcal{N}}(\pi/2 + \theta)| \sim \frac{\epsilon |\Delta T(\theta)|}{T} \quad (73)$$

We can thus extract an experimental temperature difference from the 2nd-harmonic amplitudes A_2 in the fringe shifts

$$\frac{\Delta \lambda(\theta)}{\lambda} \sim \frac{2D}{\lambda} \frac{\Delta \bar{c}_\theta}{c} = A_2 \cos 2\theta \quad (74)$$

At room temperature, say $T = 288 \text{ K} + \Delta T$, this gives the relations

$$A_2^{\text{EXP}}(\text{air}) \sim \frac{2D}{\lambda} \frac{\epsilon_{\text{air}}(T) \Delta T^{\text{EXP}}}{T} \sim \frac{2D}{\lambda} \cdot 10^{-9} \frac{\Delta T^{\text{EXP}}}{\text{mK}} \quad (75)$$

and

$$A_2^{\text{EXP}}(\text{helium}) \sim \frac{2D}{\lambda} \frac{\epsilon_{\text{helium}}(T) \Delta T^{\text{EXP}}}{T} \sim \frac{2D}{\lambda} (1.1 \cdot 10^{-10}) \frac{\Delta T^{\text{EXP}}}{\text{mK}} \quad (76)$$

The temperature differences from the various experiments are reported in Table 3.

Our calculation shows that the old estimates of $1 \div 2 \text{ mK}$ by Kennedy, Shankland and Joos (see [26]) were too large, by about one order of magnitude. At the same time, the six determinations in Table 3 are well consistent with each other as shown by the excellent chi-square, $2.4/(6 - 1) = 0.48$, of their average

$$\langle \Delta T^{\text{EXP}} \rangle = (0.26 \pm 0.06) \text{ mK} \quad (77)$$

Thus the light anisotropy observed in the classical experiments could also be explained in terms of a thermal gradient with a *non-local* origin suggesting that $\langle \Delta T^{\text{EXP}} \rangle$ might ultimately be related to the CMB temperature dipole of $\pm 3 \text{ mK}$. However, without a quantitative calculation, the fundamental energy flow expected in a Lorentz-non-invariant vacuum (see the Appendix) could represent another possible explanation. In any case, a thermal interpretation had already been deduced in refs.[28, 6] by noticing that Eq.(19) is just a special case of the light anisotropy expected from convective currents of the gas molecules associated with the

earth motion (see Appendix 1 of [6]). All this, can most easily be summarized by re-expressing the θ -dependent refractive index $\bar{\mathcal{N}}(\theta) \equiv \frac{c}{c_\gamma(\theta)}$ Eq.(17) as

$$\frac{\bar{\mathcal{N}}_{\text{gas}}(\theta)}{\mathcal{N}_{\text{gas}}} \sim 1 + (a_{\text{thermal}} + a_v)\beta^2 (2 - \sin^2 \theta) \quad (78)$$

Here $a_{\text{thermal}} \equiv (\mathcal{N}_{\text{gas}} - \mathcal{N}_v)$ and $a_v \equiv (\mathcal{N}_v - 1) \sim 10^{-9}$. In this way, for gases in normal conditions, the genuine a_v vacuum term is always numerically irrelevant and all anisotropy is due to a_{thermal} (recall that $a_{\text{thermal}} \sim 2.8 \cdot 10^{-4}$ or $a_{\text{thermal}} \sim 3.3 \cdot 10^{-5}$ respectively for air or gaseous helium at room temperature and atmospheric pressure).

7.2 Light anisotropy in solid dielectrics

Armed with this type of thermal interpretation, we can then address the second question concerning the ether-drift experiments in solid dielectrics, of the type performed by Shamir and Fox [24] in 1969. They were aware that the Michelson-Morley experiment did not yield a strictly zero result: “The non-zero result might have been real and due to the fact that the experiment was performed in air and not in vacuum” [24]. Thus, with \mathcal{N} values substantially above unity, and within the traditional Lorentz-contraction interpretation, one might expect to observe a large ether-drift $\frac{|\Delta c_\theta|}{c} \sim (\mathcal{N}^2 - 1)\beta^2 \sim \beta^2 \sim 10^{-6}$. The search for such effect was the motivation for their experiment in perspex ($\mathcal{N} = 1.5$). Since no such enhancement was observed, they concluded that the experimental basis of special relativity was strengthened.

However, with a thermal interpretation of the residuals observed in gaseous media, the two different behaviors can be reconciled. In a strongly bound system as a solid, in fact, a small temperature gradient of a fraction of millikelvin would mainly dissipate by heat conduction without generating any appreciable particle motion or light anisotropy in the rest frame of the apparatus. Hence, the non-trivial, physical difference between experiments in gaseous systems and experiments in solid dielectrics. In the latter case, we do not expect any enhancement with respect to the pure vacuum case. This means that, with very precise measurements, a fundamental vacuum anisotropy $\lesssim 10^{-15}$ should also show up in strongly bound solid dielectrics.

To see this, let us first recall that, in our picture, a relation similar to Eq.(78) is also valid in the vacuum limit where it takes the form

$$\frac{\bar{\mathcal{N}}_v(\theta)}{\mathcal{N}_v} \sim 1 + (\mathcal{N}_v - 1)\beta^2 (2 - \sin^2 \theta) \quad (79)$$

with, see Eq.(56), $(\mathcal{N}_v - 1) \sim \frac{z}{2} 1.4 \cdot 10^{-9}$ and $z = 1$ or 2 .

The existence of \mathcal{N}_v produces a tiny difference between the refractive index defined relatively to the ideal value $c_\gamma = c$ and the refractive index defined relatively to the physical isotropic value $c_\gamma = c/\mathcal{N}_v$ measured on the earth surface. The percentage difference between the two definitions is proportional to $\mathcal{N}_v - 1$ and, for all practical purposes, can be ignored.

More significantly, all materials exhibit a background vacuum anisotropy proportional to $(\mathcal{N}_v - 1)\beta^2 \sim 10^{-15}$. As explained, for gases in normal pressure conditions this genuine vacuum effect can be neglected. For solid dielectrics, on the other hand, where no thermal

enhancement is expected, one should keep track of the vacuum term. To this end, first replace the average isotropic value

$$\frac{c}{\mathcal{N}_{\text{solid}}} \rightarrow \frac{c}{\mathcal{N}_v \mathcal{N}_{\text{solid}}} \quad (80)$$

Then use Eq.(79) to replace \mathcal{N}_v in the denominator with $\bar{\mathcal{N}}_v(\theta)$ and take into account the motion of the laboratory relatively to the preferred Σ frame. This is equivalent to define a θ -dependent refractive index for the solid dielectric

$$\frac{\bar{\mathcal{N}}_{\text{solid}}(\theta)}{\mathcal{N}_{\text{solid}}} \sim 1 + (\mathcal{N}_v - 1)\beta^2 (2 - \sin^2 \theta) \quad (81)$$

so that

$$[\bar{c}_\gamma(\theta)]_{\text{solid}} = \frac{c}{\bar{\mathcal{N}}_{\text{solid}}(\theta)} = \frac{c}{\mathcal{N}_{\text{solid}}} [1 - (\mathcal{N}_v - 1)\beta^2 (2 - \sin^2 \theta)] \quad (82)$$

with an anisotropy

$$\frac{[\Delta \bar{c}_\theta]_{\text{solid}}}{[c/\mathcal{N}_{\text{solid}}]} \sim (\mathcal{N}_v - 1)\beta^2 \cos 2\theta \sim \frac{z}{2} 1.4 \cdot 10^{-9} \cdot 10^{-6} \cos 2\theta \lesssim 10^{-15} \quad (83)$$

Thus, for light propagation in solids, we would predict the same type of irregular signal discussed for pure vacuum and shown in our Fig.6. This expectation is consistent with the other cryogenic experiment by Nagel et al. [17]. In fact, most electromagnetic energy propagates in a dielectric with refractive index $\mathcal{N} \sim 3$ (at microwave frequencies) but the typical, *instantaneous* determination (see their Fig.3 b) is again $|\frac{\Delta \nu}{\nu_0}| \lesssim 10^{-15}$ as in the vacuum case (and as in the vacuum case it is about 1000 times larger than the average determination $|\langle \frac{\Delta \nu}{\nu_0} \rangle| \lesssim 10^{-18}$ obtained by combining a large number of measurements). For this reason the persistence, in vacuum and in solid dielectrics, of the irregular 10^{-15} signal should be definitely established. Instead, the present statistical averages, at the level $|\langle \frac{\Delta \nu}{\nu_0} \rangle| \lesssim 10^{-18}$, have no particular significance. With a stochastic signal, there is no problem in reaching the level $|\langle \frac{\Delta \nu}{\nu_0} \rangle| \lesssim 10^{-19}$, $|\langle \frac{\Delta \nu}{\nu_0} \rangle| \lesssim 10^{-20}$... by simply increasing the number of observations.

Finally, a complementary test could be performed by placing the vacuum (or solid dielectric) optical cavities on board of a satellite, as in the OPTIS proposal [81]. In this case where, even in a flat-space picture, the effective vacuum refractive index \mathcal{N}_v for the freely-falling observer is exactly unity, the typical instantaneous frequency shift should be much smaller (by orders of magnitude) than the corresponding 10^{-15} value measured with the same interferometer on the earth surface.

8. Summary and conclusions

The standard interpretation of the dominant CMB dipole anisotropy is in terms of a Doppler effect due to the motion of the solar system with an average velocity of 370 km/s toward a point in the sky of right ascension 168 degrees and declination -7 degrees. As discussed in the Introduction, the implications of this result may be more radical than usually believed. Indeed, the satisfactory kinematic reconstruction of the observed dipole, from the various peculiar motions which are involved, leads to the natural concept of a global frame of rest determined by the average distribution of matter in the universe. At the same time, this

global frame could also reflect a vacuum structure with some degree of substantiality and, in this sense, could characterize non-trivially the form of relativity which is physically realized in nature.

Starting from these premises, it is natural to explore the possibility to correlate ether-drift measurements in laboratory with direct CMB observations in space. The present view is that no such meaningful correlation has ever been observed. In fact all data (from Michelson-Morley until the modern experiments with optical resonators) are considered as a long sequence of null results obtained in measurements with better and better systematics.

Instead, we have argued that this present view is far from obvious. The main argument is based on a modern version of Maxwell's original calculation for the anisotropy of the two-way velocity of light. By using simple symmetry arguments, in the infinitesimal region of refractive index $\mathcal{N} = 1 + \epsilon$ a possible non-zero anisotropy should scale as $\frac{|\Delta\bar{c}_\theta|}{c} \sim \epsilon v^2/c^2$, see Eq.(19), v being the earth velocity with respect to a hypothetical preferred frame. Therefore, due to the strong suppression, with respect to the classical estimate $\frac{|\Delta\bar{c}_\theta|}{c} \sim v^2/c^2$, the size of the small residuals observed in the classical experiments in gaseous media (Michelson-Morley, Miller, Illingworth, Joos,..) can become consistent with the typical value $v \sim 370$ km/s obtained from the direct CMB observations. The essential point is contained in the relation $v_{\text{obs}}^2 \sim 2\epsilon v^2$ which connects the *kinematical* velocity v to a much smaller *observable* velocity v_{obs} which determines the magnitude of the fringe shifts.

For the full consistency of this interpretation, however, a change of perspective is needed. Namely, the irregular character of the data requires that the local velocity field v_μ which determines light anisotropy, and as such the fringe shifts in the old experiments or the frequency shifts in the modern experiments, should *not* be identified with the global velocity field \tilde{v}_μ as directly fixed by the earth cosmic motion. Instead, from general arguments related to the idea of the vacuum as an underlying stochastic medium, we have proposed that the relation between these two quantities might be indirect and similar to what happens in turbulent flows. This means that the local v_μ could fluctuate randomly while the global \tilde{v}_μ would just fix its typical boundaries. Thus, if turbulence becomes homogeneous and isotropic at small scales, one has a definite model where a genuine instantaneous signal can well coexist with vanishing statistical averages for all vectorial quantities.

In this alternative picture, the direction of the local drift in the plane of the interferometer is a completely random quantity which has no definite limit by combining a large number of observations. Therefore, one should concentrate on the positive-definite quadratic amplitude of the signal and on its time modulations. In this case, by restricting to the amplitude, the results of ref.[28] indicate a good consistency of the residuals of the classical experiments with the direct CMB observations. This alternative view should be checked with a new series of tests in which the optical resonators, which are coupled to the lasers, are filled by gaseous media. This would reproduce the physical conditions of those early measurements with today's greater accuracy. At present, a first rough check can be obtained from the time variations of a few kHz observed in the only modern experiment performed in similar conditions, namely the 1963 MIT experiment by Jaseja et. al [58] with He-Ne lasers (see the discussion given in [59]).

Waiting for these new experiments, we have compared our picture with the frequency

shift detected in modern vacuum experiments. The point is that for the physical vacuum the ideal equality $\mathcal{N}_v = 1$ might not be exact. For instance, as proposed in [42], a very tiny value $\mathcal{N}_v - 1 = \epsilon_v \sim 10^{-9}$ could reveal the different effective refractivity between an apparatus in an ideal freely-falling frame and an apparatus on the earth surface. In this case, we would expect a genuine, stochastic frequency shift $\frac{|\Delta\nu(t)|}{\nu_0} \sim \epsilon_v (v/c)^2 \sim 10^{-15}$ which coexists with vanishing statistical averages for all vectorial quantities, such as the C_k and S_k Fourier coefficients extracted from a standard temporal fit to the data with Eqs.(31) and (32).

The numerical simulations shown in Sect.6 indicate that this expectation is well consistent with the presently most precise room-temperature experiment of ref.[23] and with the cryogenic experiment of ref.[22] (which is only less precise by about a factor of 2). By itself, this substantial agreement between experiments with different systematics indicates that the observed signal might have a genuine physical component and not just originate from spurious noise in the spacers and the mirrors of the optical resonators, as assumed so far. In fact, the estimates of these contributions [80] are based on the fluctuation-dissipation theorem and thus there is no obvious reason that experiments operating at so different temperatures exhibit the same instrumental effects. The unexplained agreement with ref.[22] is particularly striking in view of the factor 100 which exists between observed signal 10^{-15} and designed short-term stability $\mathcal{O}(10^{-17})$. Tentatively, the authors of [22] interpreted this discrepancy as being due to a lack of rigidity of their cryostat but, probably, they have not considered the possibility of a genuine random signal and of intrinsic limitations placed by the vacuum structure. In this different perspective, the alternative interpretation proposed in [42], and implemented here, should also be taken into account.

This becomes even more true in view of the very good agreement obtained between the experimental value for the spread of the instantaneous signal found in ref.[23], namely $\sigma_{\text{exp}}(\Delta\nu) \sim 0.24$ Hz, and our corresponding simulated value $\sigma_{\text{th}}(\Delta\nu) \sim (0.26 \pm 0.02)$ Hz for that experiment, with $z = 2$ in Eq. (56).

The agreement we have obtained looks very promising and opens the possibility to reconstruct the CMB dipole with precise optical measurements performed within the earth laboratory and thus definitely clarify the fundamental issue of a preferred frame. To this end, however, real *data* (and not just the results of *fits*) should become available. In fact, our model, besides implying vanishing statistical averages for all vectorial quantities, in agreement with the observations, makes other definite predictions. For instance, precise time modulations of the quadratic amplitude of the signal and non-Gaussian (i.e. long-tail) distributions for the individual measurements. Although, at present, modern experiments give no information on these aspects, this idea of long tails finds definite support in the statistical analysis of Miller's extensive observations, see Fig.1 of the paper by Shankland et al. [26] reported here as our Fig.8.

Finally, in Sect.7, we have addressed the possible physical mechanism which enhances the signal in gaseous media, respectively $\frac{|\Delta\bar{c}_\theta|}{c} = \mathcal{O}(10^{-10})$ and $\frac{|\Delta\bar{c}_\theta|}{c} = \mathcal{O}(10^{-11})$ for air or helium at atmospheric pressure, relatively to the instantaneous vacuum value $\frac{|\Delta\bar{c}_\theta|}{c} \lesssim 10^{-15}$ found in modern experiments on the earth surface. For instance, one could imagine a suitable

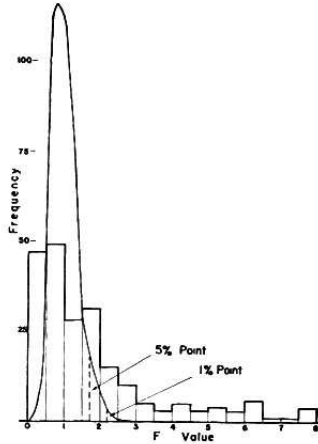


FIG. 1. The distribution of F -values for 216 sets of Mount Wilson data. The smooth theoretical curve is normalized so that the area under this curve is equal to the area of the histogram.

Figure 8: *The probability histogram for 216 sets of Miller's observations as computed by Shankland et al. [26].*

interaction of the incoming radiation with the medium to produce a different polarization in different directions. Any such mechanism, however, should act in both gaseous matter and solid dielectrics with the final result that light anisotropy should always increase with the refractivity of the medium, in contrast with the experimental evidence.

Therefore, if the enhancement observed in gases has to be specific of such weakly bound forms of matter, the natural interpretation is in terms of a *non local* temperature gradient associated with the earth motion. This shows up in all classical experiments, in agreement with the traditional thermal interpretation of the observed residuals. Only, its average magnitude $\langle \Delta T \rangle = (0.26 \pm 0.06)$ mK is somewhat smaller than the old estimates (about $1 \div 2$ mK) by Kennedy, Joos and Shankland. Conceivably, it might ultimately be related to the CMB temperature dipole of ± 3 mK or reflect the fundamental energy flow expected in a Lorentz-non-invariant vacuum state. While, at present, we have no definite quantitative insight, yet such thermal interpretation is important to understand the differences and the analogies among experiments in gaseous media, in vacuum and in solid dielectrics. Indeed, for experiments with optical cavities maintained in an extremely high vacuum (both at room temperature and in the cryogenic regime), where any residual gaseous matter is totally negligible, such tiny temperature variations cannot produce any observable effect.

On the other hand, in solid dielectrics a so small temperature gradient should mainly dissipate by heat conduction without generating any appreciable particle motion or light anisotropy in the rest frame of the apparatus. Hence, in solid dielectrics we do not expect any sizeable enhancement with respect to what is observed in the pure vacuum case. This expectation is consistent with the cryogenic experiment by Nagel et al. [17] where light propagates in a dielectric with refractive index $\mathcal{N} \sim 3$ (at microwave frequencies) but the typical, *instantaneous* determination (see their Fig.3 b) is again $\frac{|\Delta \bar{c}_\theta|}{c} \lesssim 10^{-15}$ as in the vacuum

case (and as in the vacuum case is about 1000 times larger than the average determination $|\langle \frac{\Delta \bar{c}_\theta}{c} \rangle| \lesssim 10^{-18}$ obtained by combining a large number of measurements).

At present, our prediction of a fundamental irregular signal $\frac{|\Delta \bar{c}_\theta|}{c} \lesssim 10^{-15}$ is the only explanation for this observed agreement between so different experiments, namely ref.[23] with vacuum cavities at room temperature, vs. ref.[17] performed in a solid dielectric in the cryogenic regime. The definite persistence of such signal would confirm the existence of a fundamental preferred frame for relativity and would have substantial implications for our interpretation of non-locality in the quantum theory. Once definitely established, complementary tests should be performed by placing the vacuum (or solid dielectric) optical cavities on board of a satellite, as in the OPTIS proposal [81]. In this ideal free-fall environment, the typical instantaneous frequency shift should be much smaller (by orders of magnitude) than the corresponding 10^{-15} value measured with the same interferometers on the earth surface.

Appendix

According to general quantum field theoretical arguments (see e.g. [7]), deciding on the Lorentz invariance of the vacuum state $|\Psi^{(0)}\rangle$ requires to consider the algebra and the eigenvalues of the *global* Poincaré operators P_α , $M_{\alpha,\beta}$ ($\alpha, \beta=0, 1, 2, 3$) where P_α are the 4 generators of the space-time translations and $M_{\alpha\beta} = -M_{\beta\alpha}$ are the 6 generators of the Lorentzian rotations with commutation relations

$$[P_\alpha, P_\beta] = 0 \tag{A1}$$

$$[M_{\alpha\beta}, P_\gamma] = \eta_{\beta\gamma} P_\alpha - \eta_{\alpha\gamma} P_\beta \tag{A2}$$

$$[M_{\alpha\beta}, M_{\gamma\delta}] = \eta_{\alpha\gamma} M_{\beta\delta} + \eta_{\beta\delta} M_{\alpha\gamma} - \eta_{\beta\gamma} M_{\alpha\delta} - \eta_{\alpha\delta} M_{\beta\gamma} \tag{A3}$$

where $\eta_{\alpha\beta} = \text{diag}(1, -1, -1, -1)$. In this framework, as first discussed in refs.[82, 83], exact Lorentz invariance of the vacuum requires to impose the problematic condition of a vanishing vacuum energy. As an example, one can consider the generator of a Lorentz-transformation along the 1-axis M_{01} for which one finds

$$P_1 M_{01} |\Psi^{(0)}\rangle = M_{01} P_1 |\Psi^{(0)}\rangle + P_0 |\Psi^{(0)}\rangle \tag{A4}$$

Therefore, even assuming zero spatial momentum for the vacuum condensation phenomenon, a non zero vacuum energy E_0 implies

$$P_1 M_{01} |\Psi^{(0)}\rangle = E_0 |\Psi^{(0)}\rangle \neq 0 \tag{A5}$$

This means that the state $M_{01} |\Psi^{(0)}\rangle$ is non vanishing so that the reference vacuum state $|\Psi^{(0)}\rangle$ cannot be Lorentz invariant.

The simplest consequence of such non-invariance of the vacuum is an energy-momentum flow along the direction of motion with respect to Σ . In fact, by defining a boosted vacuum state $|\Psi'\rangle$ as

$$|\Psi'\rangle = e^{\lambda' M_{01}} |\Psi^{(0)}\rangle \quad (\text{A6})$$

(recall that $M_{01} \equiv -iL_1$ is an anti-hermitian operator) and using the relations

$$e^{-\lambda' M_{01}} P_1 e^{\lambda' M_{01}} = \cosh \lambda' P_1 + \sinh \lambda' P_0 \quad (\text{A7})$$

$$e^{-\lambda' M_{01}} P_0 e^{\lambda' M_{01}} = \sinh \lambda' P_1 + \cosh \lambda' P_0 \quad (\text{A8})$$

one finds

$$\langle P_1 \rangle_{\Psi'} = E_0 \sinh \lambda' \quad \langle P_0 \rangle_{\Psi'} = E_0 \cosh \lambda' \quad (\text{A9})$$

Clearly this result contrasts with the alternative approach where one tends to consider E_0 as a spurious concept and rather tries to characterize the vacuum through a *local* energy-momentum tensor of the form [84, 85]

$$\langle W_{\mu\nu} \rangle_{\Psi^{(0)}} = \rho_\nu \eta_{\mu\nu} \quad (\text{A10})$$

(ρ_ν being a space-time independent constant). In this case, one is driven to completely different conclusions. In fact, by introducing the Lorentz transformation matrices Λ_ν^μ to any moving frame S' , defining $\langle W_{\mu\nu} \rangle_{\Psi'}$ through the relation

$$\langle W_{\mu\nu} \rangle_{\Psi'} = \Lambda^\sigma_\mu \Lambda^\rho_\nu \langle W_{\sigma\rho} \rangle_{\Psi^{(0)}} \quad (\text{A11})$$

and using Eq.(A10), the expectation value of W_{0i} in any boosted vacuum state $|\Psi'\rangle$ vanishes, just as it vanishes in $|\Psi^{(0)}\rangle$, so that

$$\int d^3x \langle W_{0i} \rangle_{\Psi'} \equiv \langle P_i \rangle_{\Psi'} = 0 \quad (\text{A12})$$

Still, the idea to simply get rid of E_0 gives rise to some problems. For instance, in a second-quantized formalism, single-particle energies $E_1(\mathbf{p})$ are defined as the energies of the corresponding one-particle states $|\mathbf{p}\rangle$ minus the energy of the zero-particle, vacuum state. If E_0 is considered a spurious concept, $E_1(\mathbf{p})$ will also become an ill-defined quantity. At the same time, the idea to characterize the physical vacuum through its energy E_0 has solid motivations. The ground state, in fact, is by definition the state with lowest energy as obtained from the solution of a minimum problem. As such, it should correspond to an energy eigenstate in view of the standard equivalence between eigenvalue equation and Rayleigh-Ritz variational procedure.

Finally, at a deeper level, one should also realize that in an approach based solely on Eq.(A10) the properties of $|\Psi^{(0)}\rangle$ under a Lorentz transformation are not well defined. In fact, a transformed vacuum state $|\Psi'\rangle$ is obtained, for instance, by acting on $|\Psi^{(0)}\rangle$ with the boost generator M_{01} . Once $|\Psi^{(0)}\rangle$ is considered an eigenstate of the energy-momentum operator, one can definitely show that, for $E_0 \neq 0$, $|\Psi'\rangle$ and $|\Psi^{(0)}\rangle$ differ non-trivially. On the other hand, if $E_0 = 0$ there are only two alternatives: either $M_{01}|\Psi^{(0)}\rangle = 0$, so that $|\Psi'\rangle = |\Psi^{(0)}\rangle$, or $M_{01}|\Psi^{(0)}\rangle$ is a state vector proportional to $|\Psi^{(0)}\rangle$, so that $|\Psi'\rangle$ and $|\Psi^{(0)}\rangle$

differ by a phase factor. Therefore, if the structure in Eq.(A10) were really equivalent to impose the exact Lorentz invariance of the vacuum, it should be possible to show similar results, for instance that such a $|\Psi^{(0)}\rangle$ state can remain invariant under a boost, i.e. be an eigenstate of

$$M_{0i} = -i \int d^3x (x_i W_{00} - x_0 W_{0i}) \quad (\text{A13})$$

with zero eigenvalue. However, there is no way to obtain such a result by just starting from Eq.(A10) (this only amounts to the weaker condition $\langle M_{0i} \rangle_{\Psi^{(0)}} = 0$). Thus, it should not come as a surprise that one can run into contradictory statements and it is not obvious that the local relations (A10) represent a more fundamental approach to the vacuum.

While a non-zero vacuum energy $E_0 \neq 0$ might have different explanations, one should also be aware that, in interacting quantum field theories, there is no known way to ensure consistently the condition $E_0 = 0$ without imposing an *unbroken supersymmetry* (which is not phenomenologically acceptable). This makes the issue of an exact Lorentz invariant vacuum a difficult problem which, at present, cannot be solved on purely theoretical grounds ¹².

¹²One could also argue that a satisfactory solution of the vacuum energy problem lies definitely beyond flat space. Nevertheless, in the absence of a consistent quantum theory of gravity, physical models of the vacuum in flat space can be useful to clarify a crucial point that, so far, remains obscure: the huge difference which is seen when comparing the typical vacuum-energy scales of particle physics with the value of the cosmological term needed in Einstein's equations to fit the observations. As discussed in Sect.5, in this perspective 'emergent-gravity' approaches [60, 61, 62, 63], where gravity somehow arises from long-wavelength excitations of the same physical flat-space vacuum, may become natural and, to find the appropriate infinitesimal value of the cosmological term, one is naturally lead [86, 87] to sharpen our understanding of the vacuum structure and of its excitation mechanisms by starting from the picture of a superfluid medium in flat space.

References

- [1] J. C. Mather, Rev. Mod. Phys. **79**, 1331 (2007).
- [2] G. F. Smoot, Rev. Mod. Phys. **79**, 1349 (2007).
- [3] M. Yoon and D. Huterer, Ap. J. Lett. **813**, L18 (2015).
- [4] G. 't Hooft, Search of the Ultimate Building Blocks, Cambridge Univ. Press 1997, p.70.
- [5] M. Consoli and P.M. Stevenson, Int. J. Mod. Phys. **A15**, 133 (2000).
- [6] M. Consoli, Found. of Phys. **45**, 22 (2015).
- [7] See, for instance, R. F. Streater and A. S. Wightman, PCT, Spin and Statistics, and all that, W. A. Benjamin, New York 1964. Plus **128**, 71 (2013).
- [8] S. Liberati, S. Sonego and M. Visser, Ann. Phys. **298** (2002) 167.
- [9] V. Scarani et al., Phys. Lett. **A276** (2000) 1.
- [10] L. Hardy, Phys. Rev. Lett. **68** (1992) 2981.
- [11] A. A. Michelson and E. W. Morley, Am. J. Sci. **34**, 333 (1887).
- [12] D. C. Miller, Rev. Mod. Phys. **5**, 203 (1933).
- [13] A. A. Michelson, et al., Ap. J. **68** (1928) p. 341-402.
- [14] K. K. Illingworth, Phys. Rev. **30**, 692 (1927).
- [15] G. Joos, Ann. d. Physik **7**, 385 (1930).
- [16] H. Müller et al., Appl. Phys. B **77**, 719 (2003).
- [17] M. Nagel et al., Nature Comm.**6**, 8174 (2015).
- [18] W. M. Hicks, Phil. Mag. **3**, 9 (1902).
- [19] A. Brillet and J. L. Hall, Phys. Rev. Lett. **42**, 549 (1979).
- [20] S. Herrmann, et al., Phys.Rev. D **80**, 10511 (2009).
- [21] Ch. Eisele, A. Newsky and S. Schiller, Phys. Rev. Lett. **103**, 090401 (2009).
- [22] M. Nagel et al., Ultra-stable Cryogenic Optical Resonators For Tests Of Fundamental Physics, arXiv:1308.5582[physics.optics].
- [23] Q. Chen, E. Magoulakis, and S. Schiller, Phys. Rev. **D 93** , 022003 (2016).
- [24] J. Shamir and R. Fox, N. Cim. **62B**, 258 (1969).
- [25] J. C. Maxwell, Ether, Encyclopaedia Britannica, 9th Edition, 1878.

- [26] R. S. Shankland et al., Rev. Mod. Phys. **27**, 167 (1955).
- [27] G. Joos, Phys. Rev. **45**, 114 (1934).
- [28] M. Consoli, C. Matheson and A. Pluchino, Eur. Phys. J. Plus **128**, 71 (2013), also arXiv:1302.3508 [physics].
- [29] M. Consoli, A. Pluchino, A. Rapisarda and S. Tudisco, Physica **A394**, 61 (2014).
- [30] R. P. Feynman, R. B. Leighton and M. Sands, The Feynman Lectures on Physics, Addison Wesley Publ. Co. 1963.
- [31] L. Onsager, Nuovo Cimento, Suppl. **6**, 279 (1949).
- [32] G. L. Eyink and K. R. Sreenivasan Rev. Mod. Phys. **78**, 87 (2006).
- [33] E. T. Whittaker, A History of the Theories of Aether and Electricity, Dover Publications, Inc. New York 1989.
- [34] O. V. Troshkin, Physica **A168**, 881-899 (1990).
- [35] H. E. Puthoff, Linearized turbulent flow as an analog model for linearized General Relativity, arXiv:0808.3401 [physics.gen-ph].
- [36] T. D. Tsankov, Classical Electrodynamics and the Turbulent Aether Hypothesis, Preprint February 2009, unpublished.
- [37] L. A. Saul, Phys. Lett. **A 314** (2003) 472.
- [38] E. Nelson, Phys. Rev. **150** (1966) 1079.
- [39] P. Jizba and H. Kleinert, Phys. Rev. **D82** (2010) 085016.
- [40] P. Jizba and F. Scardigli, Special Relativity induced by Granular Space, arXiv:1301.4091v2[hep-th].
- [41] H. Müller, Phys. Rev. D **71**, 045004 (2005).
- [42] M. Consoli and L. Pappalardo, Gen. Rel. and Grav. **42**, 2585 (2010).
- [43] V. Guerra and R. de Abreu, Eur. J. of Phys. **26** (2005) S117.
- [44] U. Leonhardt and P. Piwnicki, Phys. Rev. **A60**, 4301 (1999).
- [45] J. M. Jauch and K. M. Watson, Phys. Rev. **74**, (1948) 950.
- [46] R. J. Kennedy, Phys. Rev. **47**, 965 (1935).
- [47] J. J. Nassau and P. M. Morse, Ap. J. **65**, 73 (1927).
- [48] L. D. Landau and E. M. Lifshitz, Fluid Mechanics, Pergamon Press 1959, Chapt. III.

- [49] J. C. H. Fung et al., *J. Fluid Mech.* **236**, 281 (1992).
- [50] A. N. Kolmogorov, *Dokl. Akad. Nauk SSSR* **30**, 4 (1940); English translation in *Proc. R. Soc. A* **434**, 9 (1991).
- [51] R. Tomaschek, *Astron. Nachrichten*, **219**, 301 (1923), English translation.
- [52] A. Piccard and E. Stahel, *Journ. de Physique et Le Radium* **IX** (1928) No.2.
- [53] A. A. Michelson, F. G. Pease and F. Pearson, *Nature*, **123**, 88 (1929).
- [54] A. A. Michelson, F. G. Pease and F. Pearson, *J. Opt. Soc. Am.* **18**, 181 (1929).
- [55] F. G. Pease, *Publ. of the Astr. Soc. of the Pacific*, **XLII**, 197 (1930).
- [56] Ch. Eisele et al., *Opt. Comm.* **281**, 1189 (2008).
- [57] J. A. Stone and A. Stejskal, *Metrologia* **41**, 189 (2004).
- [58] T. S. Jaseja, et al., *Phys. Rev.* **133**, A1221 (1964).
- [59] M. Consoli, A. Pluchino and A. Rapisarda, *Europhysics Lett.* **113**, 19001 (2016), also arXiv:1601.06518 [astro-ph.CO]
- [60] C. Barcelo, S. Liberati and M. Visser, *Class. Quantum Grav.* **18**, 3595 (2001).
- [61] M. Visser, C. Barcelo and S. Liberati, *Gen. Rel. Grav.* **34**, 1719 (2002).
- [62] G. E. Volovik, *Phys. Rep.* **351**, 195 (2001).
- [63] R. Schützhold, *Class. Quantum Gravity* **25**, 114027 (2008).
- [64] M. Consoli, *Class. Quantum Grav.* **26**, 225008 (2009).
- [65] C. D. Hoyle et al., *Phys. Rev.* **D70**, 042004 (2004).
- [66] H. Yilmaz, *Phys. Rev.* **111**, 1417 (1958).
- [67] B. O. J. Tupper, *N. Cimento* **19B**, 1974 (135); *Lett. N. Cimento* **14**, 627 (1974).
- [68] R. P. Feynman, in *Superstrings: A Theory of Everything ?*, P. C. W. Davies and J. Brown Eds., Cambridge University Press, 1997, pag. 201.
- [69] R. D'E. Atkinson, *Proc. R. Soc.* **272**, 60 (1963).
- [70] K. Thorne, *Black Holes and Time Warps: Einstein's Outrageous Legacy*, W. W. Norton and Co. Inc, New York and London, 1994, see Chapt. 11 "What is Reality?".
- [71] R. J. Cook, *Am. J. Phys.* **72**, 214 (2004).
- [72] A. S. Eddington, *Space, Time and Gravitation*, Cambridge University Press, 1920.
- [73] A. M. Volkov, A. A. Izmet'sev, and G. V. Skrotski, *Sov. Phys. JETP* **32**, 686 (1971).

- [74] L. D. Landau and E. M. Lifshitz, The Classical Theory of Fields, Pergamon Press, 1971, p.257.
- [75] J. Broekaert, Found. of Phys. **38**, 409 (2008).
- [76] D. A. Jennings et al. , Journ. of Res. Nat. Bur. Stand. **92**, 11 (1987).
- [77] K. R. Sreenivasan, Rev. Mod. Phys. **71**, Centenary Volume 1999, S383.
- [78] C. Beck, Phys. Rev. Lett. **98**, 064502 (2007).
- [79] C. Tsallis, Introduction to Nonextensive Statistical Mechanics, Springer, 2009.
- [80] K. Numata, A. Kemery and J. Camp, Phys. Rev. Lett. **93**, 250602 (2004).
- [81] C. Lämmerzahl et al., Class. Quantum Gravity **18**, 2499 (2001).
- [82] M. Consoli and E. Costanzo, Eur. Phys. Journ. **C54**, 285 (2008).
- [83] M. Consoli and E. Costanzo, Eur. Phys. Journ. **C55**, 469 (2008).
- [84] Y. B. Zeldovich, Sov. Phys. Usp. **11**, 381 (1968).
- [85] S. Weinberg, Rev. Mod. Phys. **61**, 1 (1989).
- [86] G. Jannes and G. E. Volovik, JETP Lett.**96**, 215 (2012)
- [87] S. Finazzi, S. Liberati and L. Sindoni, Phys. Rev. Lett. **108**, 071101 (2012).